Faculdade de Engenharia da Universidade do Porto

Highly Sensitive Immunosensors for Degenerative Disease Biomarkers Detection

Anabela Araújo Ferreira Santos

September 2019

Faculdade de Engenharia da Universidade do Porto

Highly Sensitive Immunosensors for Degenerative Disease Biomarkers Detection

Anabela Araújo Ferreira dos Santos

DISSERTATION

Dissertation carried out under the
Master's Degree in Biomedical Engineering

Supervisor: Prof.Dra. Maria do Carmo da Silva Pereira
Co-Supervisor: Prof.Dra. Simone Barreira Morais

September 2019

Abstract

Parkinson disease (PD) is a neuropathology that appears when the *substantia nigra* pars compacta lose their dopaminergic neurons. The onset of PD possibly appears years before the first motor characteristics symptoms. All current treatments have therapeutic limitations related to the disease evolution because impairment progresses before symptoms occur. α-Synuclein (α-syn) is an important biomarker for PD. Thus, immunosensors capable of detecting PD biomarkers can help the detection, the management and the treatment of this major neurodegenerative disease.

Herein, a novel sensitive label-free immunosensor for detection of the principal biomarker of PD, α-synuclein, is described. A pyrolytic graphite electrode (PGE) was modified through the adsorption of a novel nanocomposite [multiwalled carbon nanotubes (MWCNTs)/polyethylene glycol (PEG)/gold nanoparticles (AuNPs)], bovine serum albumin and immobilization of the α-syn monoclonal antibody; the relevant experimental variables were optimized. Antibodies were functionalized through chemical modification (thiolation) in order to occur a proper and successful antibody immobilization on the nanocomposite surface, which allowed the label free detection of α-syn. Cyclic voltammetry (CV), square-wave voltammetry (SWV) and electrochemical impedance spectroscopy (EIS) were used to characterize the immunosensor development. Under the optimum conditions, α-syn was detected within the linear range of 500-20000 ng mL^{-1} with a detection and quantification limit of 8.5 and 1231 ng mL^{-1}, respectively. The proposed immunosensor enables a rapid and sensitive detection (15.2%$_{reduction}$ mL ng^{-1}) of α-syn. Still, further validation assays are needed to fully characterize the real potential applicability of the developed immunosensor.

Resumo

A neuropatologia da doença do Parkinson (DP) surge quando a *substantia nigra pars compacta* perde os seus neurónios dopaminérgicos. O início da doença começa, possivelmente, muito antes dos sintomas motores característicos da mesma surgirem. Todos os tratamentos atualmente disponíveis apresentam limitações terapêuticas, essencialmente devido à forma como a doença evolui. A α-sinucleína constitui um importante biomarcador para a doença do Parkinson. Imunossensores, capazes de detetar este e outros potenciais biomarcadores da doença de Parkinson, podem ajudar no diagnóstico, no controlo e no tratamento desta doença.

O objetivo desta dissertação consistiu no desenvolvimento de um novo imunossensor, sensível e *label-free*, capaz de detetar o principal biomarcador da DP, a α-sinucleína. Um elétrodo de grafite pirolítica foi modificado através da adsorção de um nanocompósito (composto por nanotubos de carbono de paredes múltiplas/polietileno glicol/nanopartículas de ouro), de albumina sérica bovina e da imobilização do anticorpo monoclonal da α-sinucleína. Todas as variáveis experimentais relevantes foram otimizadas. O anticorpo foi funcionalizado através de uma modificação química (a tiolação) a fim de ocorrer a imobilização adequada na superfície do nanocompósito, o que, por sua vez, permitiu detetar a α-sinucleína. As técnicas de voltametria cíclica e de onda quadrada, e a espectroscopia de impedância eletroquímica foram utilizadas para caracterizar o desenvolvimento do imunossensor. Sob as condições ótimas, a α-sinucleína foi detetada dentro da gama linear de concentrações de 500-20000 ng mL^{-1} com um limite de deteção e quantificação de 8.5 e 1231 ng mL^{-1}, respetivamente. O imunossensor proposto permite uma deteção rápida e sensível (15.2%$_{redução}$ mL ng^{-1}) da α-sinucleína. Contudo, é necessário efetuar mais ensaios de validação, a fim de caracterizar completamente o real potencial da aplicabilidade do imunossensor desenvolvido.

Acknowledgements

I would like to express my sincere gratitude to my supervisor Prof. Maria do Carmo da Silva Pereira and to my co-supervisor Prof. Simone Barreira Morais, for helping me with this project and for the learnings opportunities. I would like also to express my gratitude to Pedro Carneiro for receiving me on GRAQ, at Instituto Superior de Engenharia do Porto (ISEP) and for promptly helping me whenever it was necessary.

Moreover, I would like to give thanks to all members from GRAQ, especially to the electro-chemical group for the constant support and availability. I am also grateful to Joana Loureiro (FEUP).

Finally, I would like to give thanks to my mother, sister, friends and family for giving me the encouragement throughout this project and for their daily and irreplaceable support.

This work was financially supported by: project UID/EQU/00511/2019 - Laboratory for Process Engineering, Environment, Biotechnology and Energy – LEPABE funded by national funds through FCT/MCTES (PIDDAC) and Project "LEPABE-2-ECO-INNOVATION" – NORTE-01-0145-FEDER-000005, funded by Norte Portugal Regional Operational Programme (NORTE 2020), under PORTUGAL 2020 Partnership Agreement, through the European Regional Development Fund (ERDF).

Content List

List of Figures

List of Tables

Abbreviations, Acronyms and Symbols

List of abbreviations

α-syn	α-synuclein
Ab	Antibody
Ab_1	Primary antibody
Ab_2	Secondary antibody
Ag	Antigen
AgNPs	Silver nanoparticles
Apt	Aptamer
AuNPs	Gold nanoparticles
BSA	Bovine serum albumin
CE	Counter electrode
CNTs	Carbon nanotubes
CPSA	Chronopotentiometric stripping analysis
CPE	Carbon paste electrodes
CS	Complementary strand
CSF	Cerebrospinal fluid
CV	Cyclic voltammetry
DA	Dopamine
EDC	1-ethyl-3-(3-dimethylaminopropyl) carbodiimide
EIS	Electrochemical impedance spectroscopy
ESIPT	Excited-state intramolecular 3-hydroxyl ⇀ 4-carbonyl proton transfer
Fab	Antigen-binding fragment
Fc	Non-antigen binding fragment
GOx	Glucose oxidase
HC	Heavy chain
HC-VR	Heavy chain and variable region
HMDE	Hanging mercury drop electrodes
Ig	Immunoglobulin
IgG	Immunoglobulin G
LC	Light chain

LC-VR	Light chain and variable region
LOD	Limit of detection
LOQ	Limit of quantification
MRI	Magnetic resonance imaging
MWCNTs	Multi-walled carbon nanotubes
ND	Neurodegenerative disease
NHS	N-hydroxysuccinimide
PBS	Phosphate buffer solution
PcTS	Phthalocyanine tetrasulfonate
PD	Parkinson Disease
PEG	Polyethylene glycol
PET	Positron emission thermography
Poly-o-ABA	Poly-o-aminobenzoic acid
RE	Reference electrode
SAMs	Self-assembled monolayers
SAW	Surface acoustic wave
SERS	Surface-enhanced Raman scattering
SWCNTs	Single walled carbon nanotubes
SWSV	Square wave stripping voltammetry
SPECT	Single-photon emission tomography
SPGE	Screen-printed gold electrode
SWV	Square-wave voltammetry
TCS	Transcranial sonography
TdT	Terminal deoxynucleotidyl transferase
WE	Working electrode

List of symbols

%IR	Current reduction
R_{ct}	Randles circuit
I_p^0	Peak current before the incubation with α-syn
I_p	Peak current after the incubation with α-syn
Sy/x	Standard deviation
B	Interception of the regression line

Chapter 1

Background and Project Guidelines

1.1 - Motivation

Parkinson disease (PD) is a common neurodegenerative disease (ND) and its rapid progression results in severe disability. The global prevalence of this type of disease is 1-2 per 1000 of the population [1]. The onset of PD possible appears years before the onset of the motor symptoms of this neurodegenerative disease. All current treatments have some therapeutic limitations related to the disease evolution because impairment likely has progressed before symptoms occur. Thus, it is necessary, in future research efforts, to modify the further delaying disability and the disease progression [2], in other words, it is essential to develop techniques that allow to identify individuals at risk and prevent the first signs of the defining motor symptoms. Electrochemical immunosensors are an important tool that can support the diagnosis, and consequently, the management and the treatment of this neurodegenerative disease mainly due to their high sensitivity and selectivity [3].

1.2 – Objectives

The objective of this project was to design an electrochemical immunosensor able to detect the biomarker of the Parkinson's disease, α-synuclein. The immunosensor construction was based on a pyrolytic graphite electrode sequentially modified with i) a nanocomposite composed by multi-walled carbon nanotubes, polyethylene glycol and gold nanoparticles, ii) bovine serum albumin and iii) with α-synuclein antibody. The process of fabrication and optimization of the proposed electrochemical biosensor was divided in the following steps:

1. Optimization of Multi-walled carbon nanotubes concentration.
2. Optimization of the PEG concentration and PEG:MWCNTs.
3. Optimization of the PEG:MWCNTs:AuNPs nanocomposite.
4. Immobilization of the antibody onto the PEG:MWCNTs:AuNPs electrode (anti-α-syn/[PEG:MWCNTs:AuNPs]/PGE).

5. Detection of α-synuclein and electroanalytical performance of the prepared immunosensor.

1.3 – Dissertation Structure

The dissertation is divided into 4 chapters.

In chapter 1, the main problems of PD, the motivation, as well as, the objectives of this research are described.

In chapter 2, the theoretical information about the different topics of this report is briefly presented. Parkinson's disease and its main features, the biomarkers that allow an early diagnosis of the disease and the biosensors available to detect α-synuclein are discussed.

In chapter 3, the main characteristics of the electrochemical techniques that were used in this project are summarized.

Chapter 4 presents the section of materials and methods used in the experimental studies.

Chapter 5 concerns the presentation and discussion of the obtained results. The topics included in this chapter are the characterization steps involved in the nanocomposite fabrication, the characterization of the bovine serum albumin and antibody immobilization, and finally the detection of α-synuclein.

The last presented chapter, chapter 6, summarizes the principal conclusions of the performed work.

Chapter 2

Introduction

2.1 – Parkinson's Disease

Parkinson disease (PD) is a common neurodegenerative disease (ND) and its rapid progression results in severe disability. Parkinson disease results from a neuronal loss in the *substantia nigra*, which in turn, leads to a striatal dopamine deficiency and intracellular inclusions containing aggregates of a lipophilic phosphoprotein called α-synuclein, being that, α-synuclein is a neuropathological hallmark of this disease.

Is infrequent occurring PD in individuals under 50 years of age, however, the incidence increases sharply 5-10-fold from the sixth to the ninth decade of life [4]. The global prevalence of this disease is 1-2 per 1000 of the population [1]. This ND is twice as usual in men than in women in most populations and the main reason for this to happen is the effect of female hormones, a sex associated genetic mechanism or sex-specified differences in exposure to environmental risk factors [5].

The neuropathology of Parkinson disease include some characteristic features, namely, widespread intracellular α-synuclein accumulation and neuronal loss in specific areas of *substantia nigra* [6]. Other types of characteristics are also present, namely, motor symptoms and mental disorders. The typical motor symptoms are bradykinesia, tremor, rigidity and impaired postural reflexes and the mental disorders are mostly depression or psychosis and, also, can occur gastrointestinal dysfunction [1]. PD is related with several non-motor symptoms that add to overall disability, like cognitive impairment, disorders of sleep, and others, even if clinical diagnosis relies on the presence of bradykinesia and other cardinal motor features.

In some regions of the brain occur degeneration in certain types of neurons that are known as dopaminergic neurons. In a more initial stage of the disease, loss of dopaminergic neurons is restricted to the ventrolateral *substantia nigra* (figure 1). Sometimes, the loss of this type of neurons arise so early and before the onset of motor symptoms which leads a dramatic widespread to other dopaminergic neurons at the end-stage of the disease [7], [8].

Other neuropathology associated to the disease is the abnormal deposition of the protein α-synuclein in the cytoplasm of certain neurons, in different brain regions. The α-synuclein is the protein product of the SNCA gene and its mutation causes one of the monogenetic forms of PD. On the other hand, the accumulation of this protein forms the Lewy bodies (figure 1),

other pathologic hallmark of PD [9]. This type of pathology results from a group of neurons and neurites that presents several insertions of misfolded and aggregated α-synuclein.

The fundamental molecular pathogenesis is related to multiple pathways and mechanisms, namely, α-synuclein proteostasis, mitochondrial function, oxidative stress, calcium homeostasis, axonal transport and neuroinflammation [10].

Some treatments have become available in the treatment of Parkinson disease which is based on pharmacological substitution of striatal dopamine (L-DOPA treatment). The principal objective of the non-dopaminergic approaches is to accomplish both motor and non-motor symptoms and deep brain stimulation for those developing intractable L-DOPA-related motor complications. Thus, it is necessary, in future research efforts, modify the further delaying disability and the disease progression [2], in other words, is essential the development of techniques that allow identify individuals at risk and prevent the first signals of the defining motor symptoms.

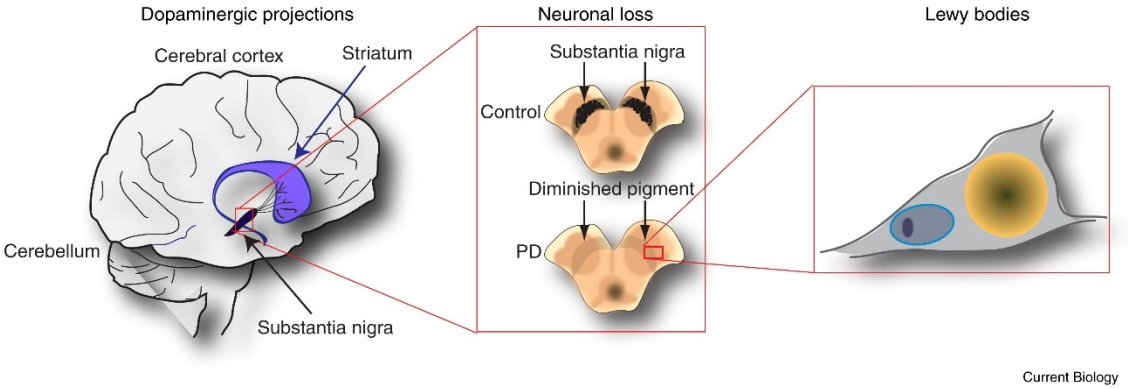

Figure 1 – Schematic representation of the neuronal loss that occurs in the *substantia nigra* of PD patients and the appearance of the Lewy bodies in their surviving cells [11].

2.2 – Biomarkers for Parkinson's Disease

It is crucial to find early diagnostic biomarkers for two principal reasons: first, to intercede at the onset of the disease and second to monitor the progress of treatments that can delay or even stop the progression of the disease.

The Biomarkers Definitions Working Group [12] has defined a biomarker as "a characteristic that is objectively measured and evaluated as an indicator of normal biological processes, pathogenic processes or pharmacological responses to a therapeutic intervention". As previously stated, there is no available biomarker that can predict the onset of PD or establishes a definitive diagnostic test. So, a useful biomarker would be reproducible, sensitive, inexpensive, and technically feasible for most laboratories, noninvasive and thoroughly validated.

Until now, α-synuclein is probably one of the most biomarkers that have been investigated [13], [14], because it appears in the brain tissue of PD patients.

Transcranial sonography (TCS), magnetic resonance imaging (MRI), single-photon emission tomography (SPECT) and positron emission tomography (PET) can establish useful and important information about structural and physiological characteristics of the brain of patients with Par-

kinson's and can also help in the clinical assessment of these patients. As these imaging techniques are non-invasive, they can constantly evaluate the integrity of the DA (dopamine) system and offer anatomical outlines, as well as information about the time frame of neuron loss. In some cases, they are correlated with the disease severity. The main neuroimaging techniques that have been used to differentiate PD from other movement disorders and to facilitate their diagnostic accuracy are MRI, functional MRI, SPECT, PET as well as transcranial sonography [15].

2.3 – Biosensors

The development and recognition of biosensors began some decades ago [16]. A biosensor can be defined as a device that uses specific biochemical reactions mediated by isolated enzymes, immunosystems, tissues organelles or whole cells to detect specific chemical compounds usually by electrical, thermal or optical signals [17].

The purpose of a biosensor is to provide reliable and accurate information, rapid and in real-time about the analyte. Ideally, it is a sensor that can reply reversibly, continuously and doesn't interfere with the sample [18]. When a biosensor is built is necessary to pay attention to some crucial factors, such as the immobilization of bioanalyte in its native configuration, the high availability of the reception sites to the species of interest, and the effectivel adsorption of the analyte to the employed support. [19].

A biosensor consists of three parts: a component that recognizes the analyte and produces a signal, a signal transducer that transfers the signal from the output domain of the recognition system, mostly to the electrical domain (bi-directional signal transfer) and a reader device, like is presented in Fig. 2. Transducers are classified according to the type of element to be recognized or according to the electrochemical transducer mode [20]. This type of sensor can be classified with several approaches [21]. Biosensors have multiple transduction principles and therefore they can be grouped as electrochemical transducers, optical transducers, mass-dependent transducers, and so on [20]. If the bioelement is considered as the basis of categorization various sets of biosensors could be acquired, namely, enzymes, nucleic acids, proteins, saccharides, oligonucleotides, ligands, etc.. Finally, if the type of detected analyte is considered as the basis of categorization innumerous biosensors could be achieved, namely, glucose, toxins, mycotoxins, drugs, classes of DNA or enzymes based [21].

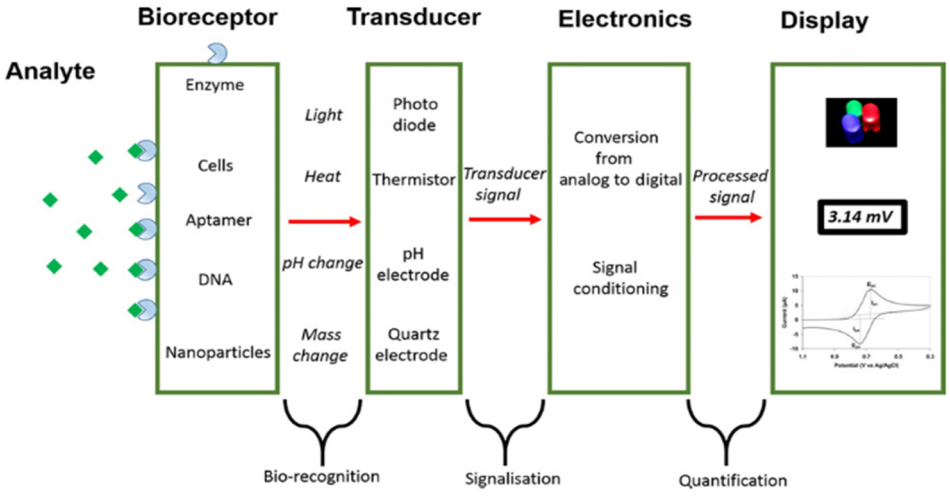

Figure 2 – Representation of the components of a biosensor [22].

2.3.1 – Electrochemical Immunosensors

An immunosensor can be described as a principle of highly specific recognition between an antibody that binds to a specific antigen (bacteria, toxins, viruses, and other biological agents) and forms a stable complex [3].

Immunosensors are an analytical type of sensor used to detect the binding event between antibody (Ab) and antigen (Ag) with the formation of a stable complex [23]. These two immunological compounds can be immobilized on the surface of different transducers and it can be a biological agent, such as, bacteria, toxins, and so on, which consequently produces a potential new immunosensor [24].

Immunosensors have different classifications, namely, they can be classified as electrochemical (voltammetric, potentiometric, conductimetric, capacitive or impedimetric, optical (luminescence, fluorescence, surface plasmon resonance, refractive index), calorimetric (based on thermistors, thermopairs or thermoresistors) and mass variation (electrochemical quartz crystal microbalance) immunosensors. This type of device has many advantages, such as, high selectivity and good sensitivity. Beyond that, immunosensors allow immunoreactions, on detector surfaces, to be monitored in real time [25].

The immunoreactions in electrochemical transducers can cause changes of potential, current, ion concentration, conductance, capacitance or impedance. Electrochemical transducers have many properties that make them widely used as immunosensors for different applications. These characteristics are generally the fact that this type of biosensor to be inexpensive, robust and with fast response times, compact, also can be mass-produced and doesn't need high volumes of analyte [24]. Being that, the electrochemical immunosensors are an important tool that can help the diagnosis of this neurodegenerative disease essentially due to their high sensitivity and selectivity [3].

2.3.2 – Nanobiomaterials-based Immunosensors

New technologies have been applied to the field of immunosensors and one example of that is nanotechnology. This type of technology is based on the manipulation of atoms or molecules at a nanoscale scale in order to achieve specific product processing and manufacturing, or simply, to study a particular material [26]. Nanomaterials have many characteristics related to their surface effects, small size effects, and macroscopic quantum tunneling effects and still evidence various unique catalytic, optical, magnetic, electrical and mechanical features [27].

Nowadays, with the rapid growth of nanotechnology a variety of nanomaterials with an outstanding performance have been developed and studied, providing an embracing platform for the construction of high-performance biosensors [26]. For instance, reducing the size of the biosensor to nanoscale allows a better signal-to-noise ratio, as well as, the possibility of using smaller sample volumes, which means lower assay costs. Moreover, when using materials with nanoscale dimensions, the surface-to-volume ratio of the sensing active area increases, and it is possible to compare the size of the detecting electrode and the size of the target biomarker. These excellent characteristics cause both reduced non-specific binding and increased binding efficiency in the target molecule [22]. As a result, it becomes possible to perform single-molecule detection [28].

An interesting fact in the interaction between an electrochemical system and nanoparticles is that the double layer capacitance intensely decreases. This phenomenon occurs due to its dependency on the electrode area. Because of the kinetic reactions that occur in this type of

nanosurfaces, it is verified that an ultra-fast electron transfer kinetics and the possibility of investigated short-life intermediate species. Moreover, it is possible to execute measurements in media with a high solution resistance where normal electrodes are not usable. In fact, it is possible to perform measurements even without the need of a supporting electrolyte [29].

Thereby, the unique properties of the application of nanomaterials based immunosensors are their ability to increase the loading amount and further enhance the reactivity, without impairing the activity of the biomolecule and the corresponding components. The electrochemical detection of analytes with nanomaterials it can greatly increase the signal and produce, consequently ultra-sensitive electrochemical immunosensors [30].

Until now, the construction of electrochemical immunosensors with different types of features have been accomplished due to the properties of nanomaterials including semiconductor (SiO nanoparticles or films), carbon-based (CNTs, mesoporous carbon, or graphene), metal-based (Au, Ag, Pt, or Cu nanoparticles or nanoclusters) and composite nanomaterials with polyethylene glycol. The more advantageous properties are their high sensitivity and stability, as well as, their low price, which leads them to present numerous applications [26]. Some of this type of nanostructures will be analyzed whit more detail in this report, namely, the gold nanoparticles (AuNPs), the carbon nanotubes (CNTs) and the polyethylene glycol and its derivatives.

The gold nanoparticles have been employed in the designing of electrochemical biosensors, essential due to their unique features, namely, their high surface-to-volume ratio and surface energy, capacity to reduce the distance between proteins and metal particles, and the ability to work as electron-conducting pathways between the electrode surface and prosthetic groups [31]–[33]. Being that, all these properties contribute to their facility in the contribution for the electron transfer between electrode surfaces and redox proteins and, therefore eliminates the necessity of using electron transfer mediators in the designing of this type of biosensors. Adding to these, they can be a useful interface in various biochemical assays for the electrocatalysis of some redox processes of specific molecules (H_2O_2, NADH, and others) [31], [34].

Concerning the synthesis of AuNPs the first method used was in 1951 by Turkevich et al. [35], where they produced these nanoparticles by treating hydrogen tetrachloroaurate with citric acid in boiling water. An important note is the fact of citrate, in this reaction, present two different functions as an agent, namely, the reducing and stabilizing function [31].

Relatively to the application of the gold nanoparticles to the electrochemical immunosensors, they play an important role, in the increasing the number of immobilized immunoreagents in a stable way, and in the enhancement of the electrochemical signal that results from the binding event between an antigen and an antibody, previously immobilized on the electrode surface [31].

In order to increase the sensibility and, consequently, the performance of a biosensor has been developed different signal amplification strategies, namely, strategies involving carbon nanotubes (CNTs) [36].

Historically, CNTs were founded in the 20th century and they can be defined as an allotropic form of carbon associated to the fullerene family [37]. They are cylindrical large molecules consisting of a hexagonal arrangement of hybridized carbon atoms [38].

CNTs can be divided into two different forms: single-walled carbon nanotubes (SWCNTs) formed by rolling up a single sheet of graphene and multi-walled carbon nanotubes formed by rolling up multiple sheets of graphene [38]. The last one was the first one to be discovered and are significantly easier to produce when compared to SWCNTs.

The application of this type of nanomaterials in electrochemical biosensors is essentially due to their unique properties: excellent mechanical strength [39] and electrical conductivity, high surface area [40] and thermal conductivity and the fact that they can be electrochemically stable in aqueous and nonaqueous solutions [36], [41]. Being that, some of these properties will be reflected in an increasing of the electron transfer and in the number of functional units immobilized on the CNT-modified electrode.

Another important aspect to consider, in the development of immunosensors is the properly immobilization of antibodies in the electrode surface. Whereby, the use of functionalized CNTs can allow this phenomenon to occur and can turn these nanostructures more biocompatible [36], [42]. Thus, electrochemical biosensors based in the CNTs nanostructured are known for presenting low manufacture cost, high sensitivity, quicker respond, ease of operation and promising portability [36].

2.3.3 – Polyethylene Glycols and PEG Derivatives

Polyethylene glycols (PEG) are synthesized from ethylene oxide and characterized as hydrophilic oligomers or polymers, which in turn, leads to a diminution of the process of aggregation and, consequently, increases the stability of proteins. PEG hold the ability to attach their terminal sites to various types of functional groups, functioning as a binder of biomolecules, which obviously, expand their benefits to other biomedical applications, like the development of biosensors [43], [44].

Whenever occurs a covalent grafting of a PEG derivative onto molecules verifies an enhancement of the water solubility, this process is known as PEGylation [45].

The PEG derivatives are commonly divided into two different groups: the bifunctional PEG derivatives and the multi-arm PEG derivatives. The last one is often associated to the formation of hydrogels [45], while the first one is mostly employed for the PEGylation of nanoparticles [46], small molecules [47], peptides [48]–[50] and proteins [46], [51]. Beside this classification, the bifunctional and the multi-arm PEG derivatives can also be divided into hetero- and homo-bifunctional PEG derivatives and into hetero- and homo-functional multi-arm PEG derivatives [52].

PEG can be a valuable component to be applied in the construction of an immunosensor by contributing with a higher number of functional antibodies in an immunoassay. They can accomplish this feature by allowing the preservation of a higher immunoglobulin affinity and by presenting a bigger number of paratopes accessible for recognition of the target [53].

Recently, D. W. Baker et al. developed an electrochemical immunosensor for human chorionic gonadotropin based on a nanocomposite constituted whit carbon nano-onions, AuNPs and PEG [44]. In this work, for the first time, PEG was applied to produce a nanocomposite composed with AuNPs and carbon nano-onions where functionalized as a binder between these two nanomaterials in a hydrophilic environment and allowing a proper antibody immobilization [44].

Thus, PEG when applied to the construction of a biosensor and, consequently, of an immunosensor, can provide more stability to the antibody and to the same time functionated as a binder between two different nanomaterials, accomplishing a highly sensitive and selective detection [44], [53].

2.3.4 – Antibody-antigen Interaction

An antibody-antigen interaction is a basic principle that involves a specific type of bio-affinity biosensor called immunosensor.

Antibodies are glycoproteins with the capacity to recognize antigens with high specificity, also known as immunoglobins (Ig). Usually, the human being has five different classes of glycoproteins (IgA, IgG, IgM, IgD, and IgE) being that the IgG class of antibody are the most used in immunoassays, essentially due to their greater affinity and specificity to bind antigens, when compared whit the other classes of antibodies referred previously [54], [55].

Antibodies can be classified in two types, monoclonal and polyclonal, depending on the region on the epitope. The first one is more specific for a single epitope and are produced by cloned cell line, which in turn reduces the probability of occurring cross-reactivity. Comparatively to the monoclonal Ab, the polyclonal antibody is able of binding to multiple epitopes on a Ag, demonstrating a heterogeneous immunological response [3], [56]. It is possible to verify that monoclonal antibodies demonstrated higher sensitivity and selectivity when compared to polyclonal antibodies. Obviously, the choice of the type of antibody will be determined by its analytical application. However, monoclonal antibodies are more suitable for the use in immunosensors [3], [57].

In the figure 3 are represented the heavy and light chains of an antibody and their 'Y' shape structure. Each 'Y' of an antibody is constituted by four polypeptide chains that divide into two identical light chains (LC) and two identical heavy chains (HC). In turn, each light and heavy chain is connected by a single disulfide bond (-SS-). In general, an antibody can be separated into two main parts, the non-antigen binding fragment (denoted as Fc) and the antigen-binding fragment (denoted as Fab). The antigen binding occurs between the heavy chain and variable region (HC-VR), and the light chain and variable region (LC-VR) [3], [58].

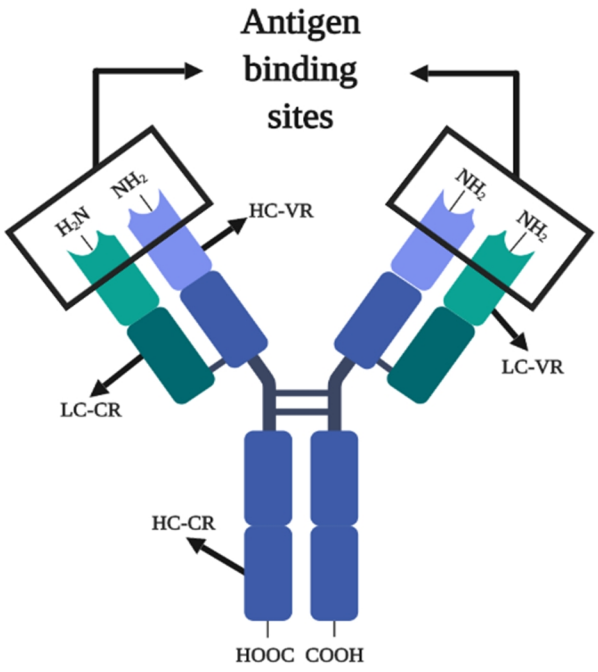

Figure 3 – Schematic representation of heavy and light chains of an antibody and theirs's 'Y' shape.

2.3.5 – Immunoassays

Immunoassays are a quantitative analytical technique where antibodies are the primary binding agents for the antigen (which is often the analyte) of interest. The technique relies on two different basic principles: on the determination of occupied sites or, indirectly, on measuring unoccupied sites. These two principles are associated with two different immunoassay formats: the competitive and non-competitive immunoassays [55].

In a competitive immunoassay, occurs a competition for a limited number of antibody-binding sites between the sample analyte and the labelled analyte, previously mixed [55], [59]. The determination of the amount of labeled analyte that interacts at the binding sites allows accomplishing a quantitative analysis with this type of immunoassay format [55].

Competitive immunoassays (figure 4) can present three different configurations: the immobilized antibody approach, the anti-immunoglobulin-coated solid phase, and the immobilized antigen approach. In the first one (Figure 4-A), the analyte from the sample competes with labeled analyte for a limit number of antibody binding sites. Relatively to the second one (figure 4-B), is used an anti-immunoglobulin-coated solid phase to capture the anti-analyte antibody. To finish, in the last one (figure 4-C), the immobilized analyte competes with the analyte from the sample for binding to labeled antibody molecules. In all configurations, the electrochemical signal obtained is inversely related to the analyte concentration [59].

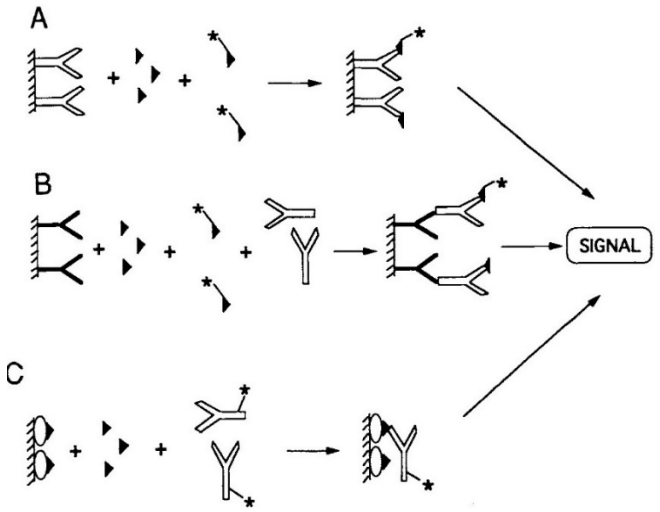

Figure 4 – Approaches for competitive immunoassays [59].

On the contrary, in a non-competitive immunoassay (figure 5), also called two-site (sandwich-type immunoassay), an excess of a capture antibody captures the sample analyte, separating it from the bulk sample. Then, the capture antibody is exposed to an excess of the second antibody, which will only bind, if the capture antibody-analyte complex was formed previously [55], [59]. Consequently, in this type of immunoassay format the measurement of the labeled analyte is directly proportional to the amount of antigen present in the sample, thus resulting that the correspondent electrochemical signal obtained increases with the increasing target analyte [60], [61].

Analyzing these two types of immunoassay formats is expected that the sandwich-type format will be the format that gives the highest level of sensitivity and specificity. Therefore, the

sandwich-type immunoassay is one of the most current configurations in immunosensings and immunoassays [59], [61].

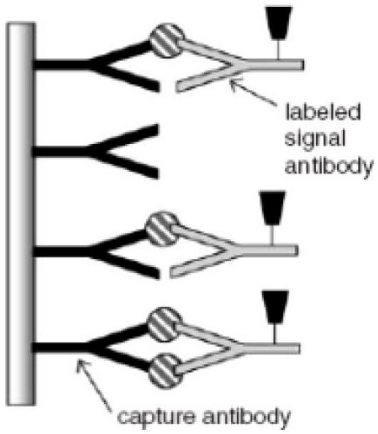

Figure 5 – A configuration of a two-site (sandwich type) immunoassay format. Adapted from [55].

2.3.6 – Antibody Immobilization Techniques

The immobilization process in the construction of an immunosensor constitutes a crucial step, that will determine the detection sensitivity, reproducibility and other bioanalytical parameters of the immunoassay, whether it is competitive or non-competitive [62].

In the last decades, have been created a wide range of antibody immobilization techniques. The first technique that was developed involve the adsorption of an antibody onto a substrate, after a prolonged incubation by passive adsorption. In the intent to circumvent critical shortcomings of the passive adsorption procedure, were developed new techniques of immobilization based on functionalization and cross-linking strategies [62]. These include physical immobilization, covalent immobilization, self-assembled monolayers (SAM) and oriented immobilization.

Physical adsorption of antibodies onto traditional substrates is executed via hydrophobic, electrostatic, or van der Waals interactions [62], [63], with a simple attachment pathway. Nevertheless, this simplest and cost-effective strategy has several limitations, such as it is uncontrollable, and antibodies can be immobilized in a randomly oriented manner, displace in later steps or, even denatured [63], [64].

The most common method for antibody immobilization for fabricating various immunosensors is the covalent cross-linking of antibodies on chemically-activated solid surfaces. Covalent attachments are habitually formed between the properly modified substrates and the available functional groups homogeneously located at the surface of proteins, creating efficient and irreversible attachment [65]. Typically, the transducer substrates have some lack of an amount of active covalently binding sites which is necessary to precoating their bases with thin films for covalently binding the antibodies or antigen, for that commonly are used functional reagents such as glutaraldehyde, carbodiimide succinimide ester, maleimide, and periodate [66]. The covalent coupling antibodies have some advantages, comparably with physical adsorption, namely guaranties a robust immobilization and can improve the orientation outcomes at the substrate and their density. Yet, is necessary a site-directed attachment to the antibody, for an oriented immobilization [63].

Self-assembled monolayers (SAMs) provides an attractive method for modifying surface chemistry, to promote antibody adsorption or to produce functional groups for subsequent covalent attachment [67]. SAMs are habitually developed from molecules that contain active functional head-groups at either a linear carbon chain and at the end of a hydrocarbon chain which allows self-assembly when they attach to a surface [63]. The central hydrocarbon chains are able to interchain hydrophobic interactions, providing a stabilization of the SAM [68]. Customizable chemistry for coupling antibodies to SAMs or adsorption can be accomplished by the gold-thiol interaction, that is the result of the use of alkanethiols and provides a linker that can bind gold substrates via the thiol group [69], [70].

Oriented immobilization means that with a proper strategy, the site-directed immobilization may be executed through a non-functional site, originating in a homogeneous antibody attachment with the desired orientation [65]. A strategy that allows a proper orientation is the 1-ethyl-3-(3-dimethylaminopropyl) carbodiimide (EDC)/N-hydroxysuccinimide (NHS) method. This method is responsible for convert antibody into NHS ester intermediate, which is highly reactive, forming a peptide bond with amine functionalized surface, facilitating the process of immobilization [71]. So, with this technique of immobilization is possible to accomplish a higher antigen binding capacity when compared to randomly oriented antibodies, essentially due to the fact that their antigen binding sites are well exposed to the solution phase [72], [73].

2.3.7 – Electrochemical Biosensors for α-synuclein

After a careful and extensive analysis of scientific papers on several databases, eight papers related to biosensors for α-synuclein were found [74]–[82], however only three papers are related to electrochemical immunosensors for detecting this biomarker [80]–[82]. Table 1 summarizes the most important analytical parameters of the reported biosensors for this biomarker.

Michal MasaroeÌk et al. [74] developed an electrochemical biosensor that according to them constitutes the first biosensor based on electrochemical methods that was applied in the study of α-synuclein, in their both forms, native and aggregated. The study of these both forms of α-syn was accomplished by using a current chronopotentiometric stripping analysis (CPSA), that was responsible for measuring the hydrogen evolution catalyzed by α-syn (peak H) applied at hanging mercury drop electrodes (HMDE). Relatively to the monitorization of the process of oxidation of tyrosine at carbon paste electrodes (CPE), the researchers used the square-wave stripping voltammetry (SWSV). The authors accomplished a subnanogram detection of α-synuclein, by using electrochemical methods, which they suggest that electrochemical methods may constitute an important key in the detection of early modifications in the aggregation process of α-synuclein and probably in other in vitro peptides and proteins.

Dmytro A. Yushchenko et al. [75] introduced a new type of technology where sensor molecules are a result of covalent adducts of Ala-to-Cys mutants of α-syn with a thiol-reactive (maleimide) probe (MFC) based on 2 (2furyl)-3-hydroxychromone. These improved tools are representative of the excited-state intramolecular 3-hydroxyl → 4-carbonyl proton transfer (ESIPT) probes of amyloid aggregation, with the capability of monitoring α-synuclein aggregation in vitro and in vivo, which leads to an unprecedented level of sensitivity for the initial stages of this reaction. Once again, this innovative sensor can be applied on several platforms and will constitute useful tools for newly related constructs that will be able to screen inhibitors or reverses of AS aggregation, as well as other proteins.

Mihaela Dragusanu et al. [76] described an on-line combination that can recognize the immobilized anti-α-syn–human/α-syn complex on a biosensor chip. The on-line combination is the result of the conjugation of a surface acoustic wave (SAW) biosensor with an electrospray ionization mass spectrometry (SAW-ESI-MS). Hence, this system can simultaneously identify and quantify the interactions between a protein and a ligand. The quantification accomplished with this on-line combination goes from micro-to low nanomolar sample concentrations, constituting a sensitive tool for label-free detection, identification, and quantification of α-synuclein and biopolymer-ligand interactions.

Daekyun Lee et al. [77] created a biosensor with surface-enhanced Raman scattering (SERS)-active AuNPs, that were individually isolated with an ultrathin α-synuclein shell. The 2-D array formed, was put into a tightly packed monolayer on a glass support, which allows a quantitative SERS measurement of phthalocyanine tetrasulfonate (PcTS), a chemical ligand of the pathological related protein of α-synuclein. Furthermore, and due to the duality of this strategy, this biosensor could be further developed in a custom-made system for the detection of biochemical reactivities of specific ligands of the immobilized coat proteins and can be used in areas including the photoelectroconductive, photocatalytic, and photodynamic effects of PcTS.

K. Sun et al. [78] reported a label-free detection of the α-synuclein oligomer, using an impedance detection by electrochemical impedance spectroscopy. The reported biosensor uses a DNA aptamer as the bioreceptor and gold nanoparticles as the signal amplifiers. The EIS principle of this aptasensor occurs as the result of the specific binding of the α-synuclein oligomer to the aptamer immobilized onto the gold working electrode surface, which in turn increase one of the parameters of this technique, the electron-transfer resistance parameter. The detection limit obtained with this biosensor was the 1 pM. In addition, the interference studies realized demonstrated that the EIS biosensor exhibits an extraordinary selectivity for the α-synuclein oligomer, therefore constituting a potentially key and a viable alternative for easy clinical diagnosis of PD.

S. M. Taghdisi et al. [79] describes a novel aptasensor able to detect the oligomers of α-synuclein. The novel biosensing platform is based on methylene blue, exonuclease I (Exo I), a screen-printed gold electrode (SPGE) and a nontarget-induced increase of the size of a label-free aptamer (Apt) and its complementary strand (CS) triggered by terminal deoxynucleotidyl transferase (TdT). For preventing that occurs an aptamer SAM aggregation and the aptamer doesn't lose their function, the CS was covalently immobilized on the surface of SPGE. The principal basic mechanism of detection is based on the accumulation of methylene blue on the surface of the working electrode. So, in the absence of α-syn oligomer, the TdT increases the lengths of Apt and CS, which increases the accumulation of methylene blue as a redox agent and, consequently results in a stronger current signal. On the other hand, in the presence of α-syn oligomer, Exo I digests CS on the electrode surface, leading to less accumulation of methylene blue and, consequently creates a weak current signal. This novel electrochemical aptasensor presented a limit of detection (LOD) of 10 pM. In addition, the aptasensor presented a high precision and repeatability for the detection of α-synuclein in serum samples. Still, and contrary to the biosensors presented above for α-synuclein, this analytical technique has more costs, essentially due to the TdT enzyme, and higher detection time. Another important feature and similarly to what happened in the other biosensors, this electrochemical technique can be simply applied to the detection of other proteins, by just replacing the Apt and its CS.

In the field of immunosensors able to detect the biomarker of the PD, Yauri An et al. [82] developed a photoelectrochemical immunosensor based on Au-doped TiO_2 nanotube arrays.

They used an anodic oxidation technique to highly order the arrays and, after that, AuNPs were photoelectrochemically deposited in the TiO_2 nanotubes. The analytical principle involves an immunoreaction between an antibody and an antigen, with a sandwich process where the primary antibody (Ab_1) immunoreacts with the target (α-syn), followed by the attachment of bioconjugates, namely, the secondary antibody (Ab_2) and the glucose oxidase (GOx) labels linked to AuNPs ({Ab_2-Au-GOx}). Relatively to the principle of detection, the concentration of the analyte was proportional to the photocurrents, with a limit of detection of 34 pg mL^{-1}. The sandwich immunoassay described presented high sensitivity, excellent stability, and acceptable reproducibility. Obviously, and like the other biosensors described here, this method could become a promising technique for protein detection, in clinical and biological analysis.

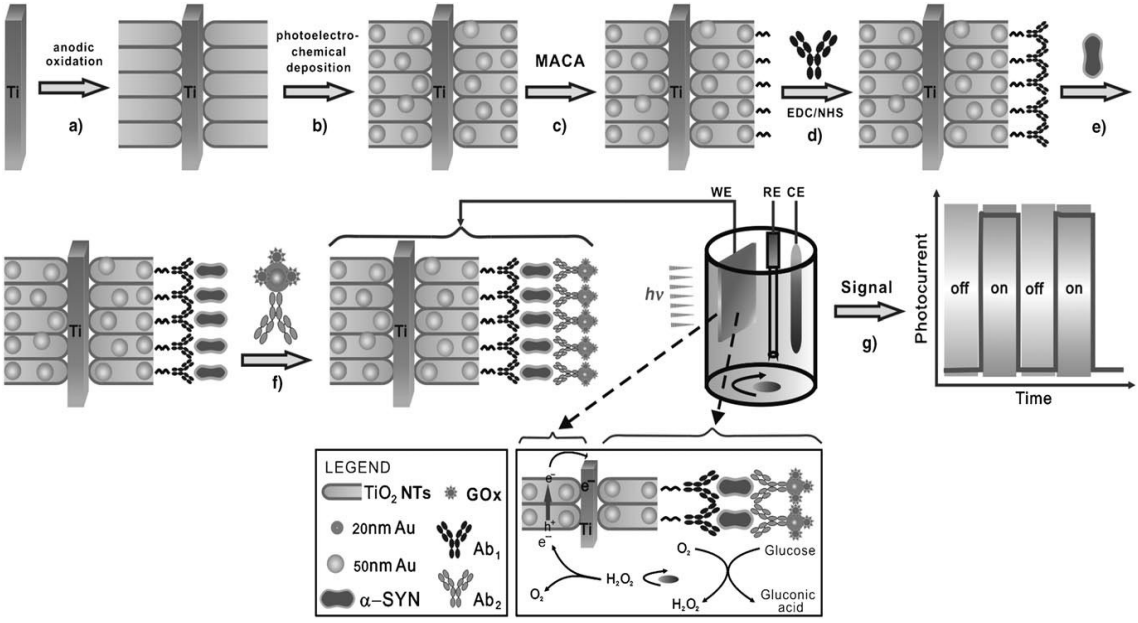

Figure 6 – Schematic representation of the steps involved in the construction of the photoimmunosensor developed by Yauri An et al. [82].

As an improvement of the work executed and describe above, in the following year, the same authors, Yauri An at al. [81] design an electrochemical immunosensor, but with different features and components. In the design of this immunosensor platform, they resorted to a strategy that had a dual signal amplification. To this strategy are included the covalent bond between the G4-polyamidoamine dendrimer-encapsulated Au nanoparticles (PAMAM-Au nanocomposites) and the poly-o-aminobenzoic acid (poly-o-ABA), which was preciously electropolymerized on the glassy carbon electrode surface to produce abundant carboxyl groups. The proposed method presented a linear range from 20 pg mL^{-1} to 200 ng mL^{-1} and a limit of detection of 14.6 pg mL^{-1}, demonstrating an excellent performance with high stability and sensitivity in the detection of α-synuclein. Furthermore, the authors believe that also this immunosensor could offer an important promise for both clinical and biological assays in a wide range of important proteins.

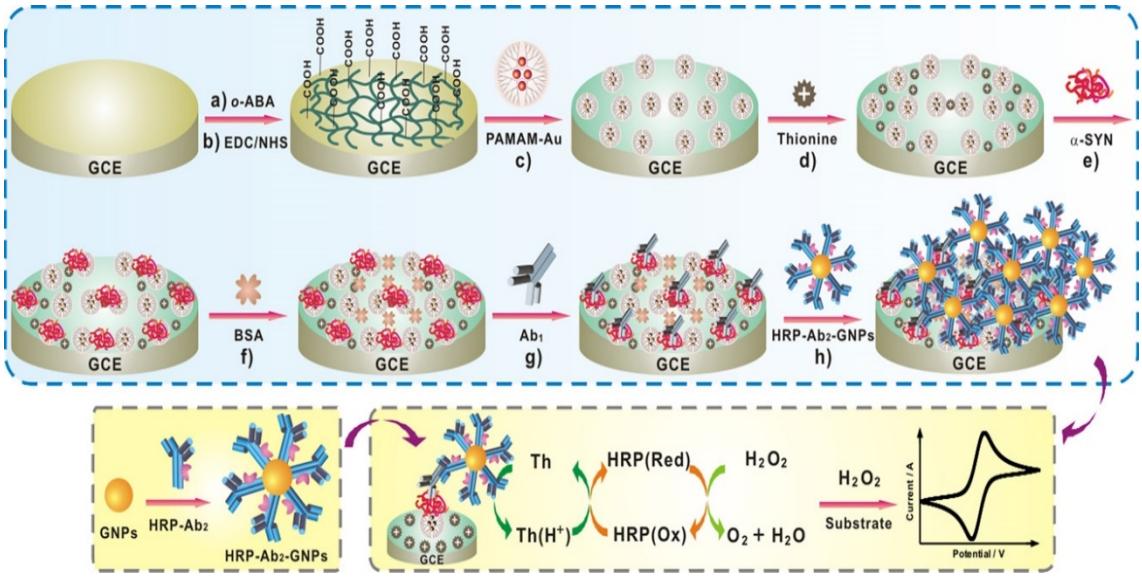

Figure 7 – Schematic representation of the steps involved in the construction of the electrochemical immunosensor developed by Yauri An et al. [81].

M. N. S. Karaboğa et al. [80] developed a disposable neuro-biosensing system that contains a gold nanoparticle (AuNP)–polyglutamic acid (PGA)-modified indium tin oxide (ITO)-based able to detect α-synuclein. It is also important to refer that, the ITO electrodes were also coated with PET films to increase the performance of the working electrode. In this work, they resorted to three different electrochemical techniques, namely, to electrochemical impedance spectroscopy, cyclic voltammetry and square wave voltammetry for designing the immobilization procedure, the optimization of the parameters that can affect the performance of the biosensor, and the analytical performance of the system. The gold nanoparticle-doped and polyglutamic acid-modified biosensing platform permitted to achieve a limit of detection of 0.135 pg mL^{-1} for the analyte. In addition, this disposable system presented other important advantages, namely, long storage stability, reproducible results, suitable components where it is possible to perform other types of modifications, and high selectivity and sensitivity for α-synuclein in the cerebrospinal fluid (CSF).

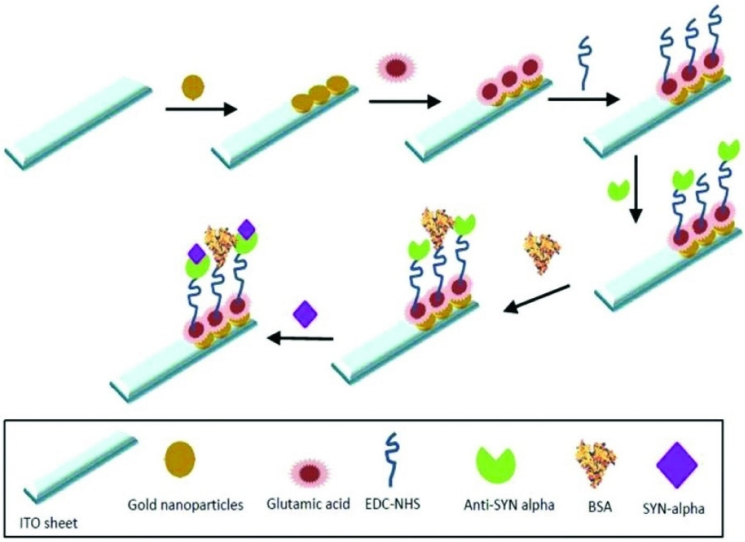

Figure 8 – Schematic representation of the steps involved in the construction of the biosensor developed by M. N. S. Karaboğa et al. [80].

Table 1 –Analytical methodologies of the most recent reported biosensors for α-synuclein. The criteria was based on the transducer, immobilization procedure, assay format, type of detection and limit of detection.

Transducer	Immobilization	Assay format	Detection	LOD	Year	Ref.
Au-doped TiO_2 nanotube arrays	Mercaptopropionic acid / EDC / NHS	Sandwich	Photo-electrochemical	34 pg mL^{-1}	2010	[82]
Glassy carbon electrode	poly-o-ABA / EDC / NHS/ PAMAM-Au/ thionine/ anti-α-synuclein / Horseradish peroxidase-labeled goat anti-mouse IgG	Sandwich	Electrochemical Impedance Spectroscopy	14.6 pg mL^{-1}	2011	[81]
Thiolated aptamer gold electrode	AuE/ thiolated aptamer / tris(carboxy-ethyl)phosphine (TCEP) / 6-mercapto-1-hexanol (MCH) / AuNPs	Sandwich	Electrochemical Impedance Spectroscopy and Colorimetric Surface Plasmon Resonance	1 pM	2017	[14]
AuNP- PGA doped ITO electrode	ITO/ AuNPs/ PGA / EDC / NHS / anti-alpha-SYN	Sandwich	Electrochemical Impedance Spectroscopy and Square Wave Voltammetry	0.135 pg mL^{-1}	2018	[80]
SPGE	SPGE / TCEP-treated 5'-Thiol CS**/ Apt / MCH / α-syn oligomer/ Exo I/ TdT/ dTTP / methylene blue	Competitive	Differential Pulse Voltammetry	10 pM	2019	[79]

Chapter 3

Electrochemical Concepts

3.1 – Electrochemical Techniques

Electrochemical techniques are a powerful tool to explore reactions involving electron transfers. They establish a relation between the flow of electrons and chemical changes, which occur in given moment. These features allow the evaluation of compositions and the kinetics of charge transfer processes, what in turn, offers a systematic and an analytical instrument to scientist [83], [84]. It is usually implemented as a complementary technique to separation and spectrophotometric techniques. These occur, due to its high sensitivity, accuracy, the speed of analysis, reduction in solvent and sample consumption, and low operating cost compared to other analytical methods [85].

Analyses based in electrochemistry commonly involve the use of three-electrode setup. In this setup, the electrodes represent a working electrode, counter electrode, and reference electrode, in contact with an electrolyte [83].

The working electrode (WE) is responsible for carrying out the electrochemical event of interest, in other words, is where the reaction of interest happens. In this type of technique is necessary to use a potentiostat to control the potential that will be applied to the electrochemical cell [83].

The counter electrode (CE) is used in an electrochemical cell to complete the electrical circuit and the flow between the WE and CE is saved as a current parameter. There is an important difference between the WE and the CE that doesn't allow the inhibition of the reaction between these two electrodes, and this difference is the fact that the WE has a minor surface area, compared to the surface area of the CE. The most used counter electrodes are the platinum disk or wire, and carbon-based counter electrodes sometimes are also used [86].

The last component that also is used in the electrochemical cell is the reference electrode (RE) and it is characterized by having a well defined and stable equilibrium potential. The RE allows the measurement of the potential of the other types of electrodes by being the point against which the potential is established. The saturated calomel electrode, the standard hydrogen electrode, and the AgCl/Ag electrode are typically used as RE [83].

The electrochemical techniques that I will use in my dissertation are the cyclic voltammetry, the square-wave voltammetry and the electrochemical impedance spectroscopy.

3.1.1 – Cyclic Voltammetry

Cyclic voltammetry is a powerful and widely electrochemical tool, usually used to analyze the reduction and oxidation processes of molecular species. CV is also precious in the study of electron transfer-initiated chemical reactions, which contains the process of catalysis. In other words, this electrochemical technique allows the obtaining of qualitative information about electrochemical reactions [83], [87].

This type of technique is potentially controlled in which the direction of the potential is reversed at the end of the first scan. The results are presented as a voltammogram where is possible visualize current against voltage and obtain information concerning the oxidation and reduction reactions. The CV scan has two important and useful parameters that are the peak potentials and the magnitude of the peak current [85].

The rate of change of potential with time is a parameter of CV, named scan rate. In an electrochemical experiment, it is possible to control how fast is scanned the applied potential, through this CV parameter. So, for example, if we intended to use faster scan rates, this will lead to an increase in current because the size of the diffusion layer is decreasing [83], [88]. Additional, CV allows you to obtain mechanistic and kinetic properties of chemical reactions when electron transfers are coupled to this type of reactions. Sometimes, this information can help in establishing the kinetics and the mechanism by which a homogeneous reaction is occurring [83], [87].

In the forward scan and in the backward scan appears two different peaks, the cathodic peak, and the anodic pick, respectively. For a reversible reaction, the magnitude of cathodic and anodic peaks currents is equal ($|i_{pc}|=|i_{pa}|$). When the reversibility of the reaction decreases there's an increase in the difference between the two peak [89], as shown in figure 9.

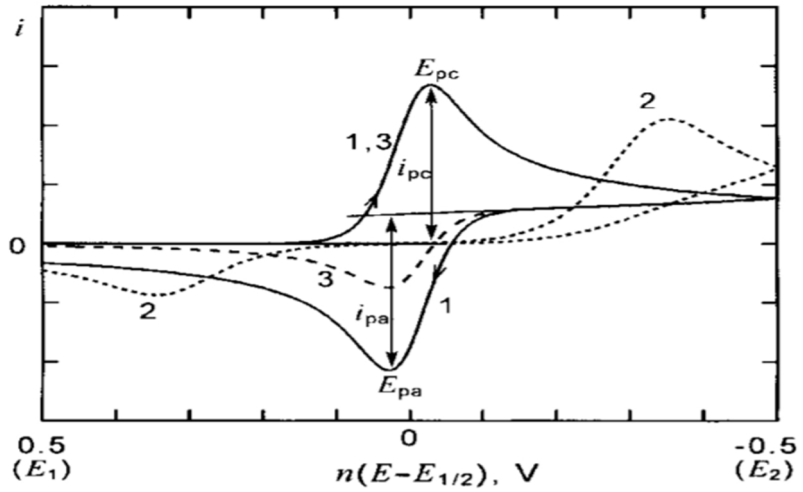

Figure 9 – Cyclic voltammograms for reversible case (curve 1) and for irreversible case (curve 2), (Parameters, n.d.) [89].

3.1.2 – Square-Wave Voltammetry

Square-wave voltammetry emerged due to recent developments in computer-controlled electroanalytical instruments. Their application boomed in the last decade essentially due to its high sensitivity to surface-confined electrode reactions [90]. The square wave voltammetry is characterized by being able to combine the advantages of other electrochemical techniques, such as cyclic voltammetry, impedance techniques. [91].

In figure 10, it is possible to verify that the staircase step coincides with the forward pulse of the square wave, and also is possible to verify the existence of a symmetrical square-wave pulse superimposed on a staircase waveform, forms the excitation signal in SWV. To the difference between the forward and reverse currents is called the net current which is adjusted the redox potential. SWV is very sensible in that it allows detecting very low concentrations (until 10^{-8} M) and the peak height presented in the voltammogram, of this method, is directly proportional to the concentration of the species that are being analyzed. [90], [91].

The Square-wave voltammetry can be applied to several types of studies, namely, on the study of the electrode kinetics and in the electrochemical detection [91].

As mentioned above, SWV results from combining the advantages of other electrochemical techniques leading to unique advantages. These advantages are their capacity to reject the background currents and the speed of the process, which allows the execution of experiments repetitively [91].

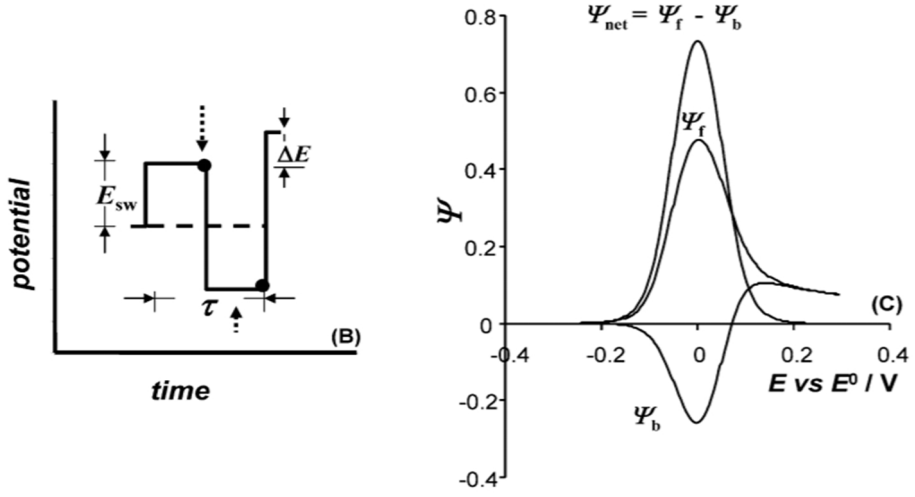

Figure 10 – Potential Cycle (B) and typical voltammogram in Square-Wave Voltammetry (C), (Parameters, n.d.) [91].

3.1.3 – Electrochemical Impedance Spectroscopy

Electrochemical Impedance spectroscopy allows a direct binding and a label-free detection. These method studies phenomena that are occurring on the surface of the system and the alterations of the bulk properties. EIS has several applications, however, it has been applied majorly in biosensors, in particular in the detection of binding events on the transducer surface [92].

The EIS allows the application of an AC potential that will perturb the system, leading the current to flow through all components of the system, including, the WE and CE, the biological material and the solution. The sum of the individual contributions of these components gives the measured impedance [92], [93].

Despite all the advantages mentioned above, EIS is time-consuming and not always needed, because exists other electrochemical methods that can give a rapid analytical response. So, EIS has preferentially used as an impedimetric technique.

The Randles circuit, showed in figure 11, is constituted by capacitors and resistors. In this figure, R_{ct} represents the charge-transfer resistance; C_d represents the double-layer capacitance; W represents the Warburg impedance and R_Ω represents the electrolyte resistance or the high-frequency series resistance. In figure 12 is showmen a typical Nyquist plot of the Randles impedance that provides a visual insight into the systems dynamics. The semicircle is represented for higher frequencies values and, the lower frequencies values are represented as a straight line, with an angle of 45° to the real axis. [94].

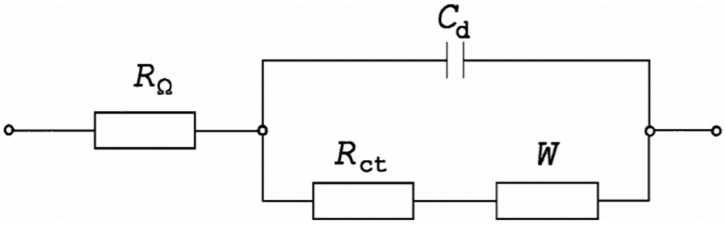

Figure 11 – Randles equivalent circuit [94].

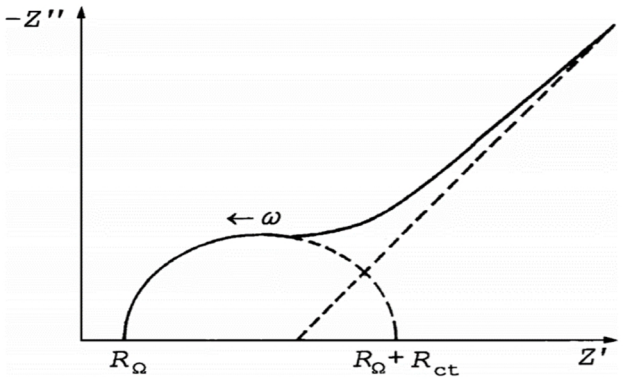

Figure 12 – Scheme of the impedance of the Randles equivalent circuit in the complex impedance [94].

Chapter 4

Materials and Methods

4.1 – Materials

Mouse monoclonal α-Synuclein (1 mg mL^{-1}) IgG (ab27766) was purchased from Abcam (U.K.). Sulfuric acid (H_2SO_4; 98%), and absolute ethanol were purchased from Panreac (Spain). Potassium nitrate (KNO_3) was purchased from Pronalab (Mexico). Potassium ferrocyanide ($K_4[Fe(CN)_6]\cdot 3H_2O$), potassium ferricyanide ($K_3Fe(CN)_6$), potassium hydrogen phosphate (K_2HPO_4), potassium phosphate monobasic (KH_2PO_4) and sodium phosphate dibasic (Na_2HPO_4), sodium chloride (NaCl), tri-Sodium citrate-2-hydrate ($C_6H_5Na_3O_7\cdot 2H_2O$; 99.5%) and potassium chloride (KCl) were purchased from Riedelde Haën (Germany). Human antigen α-Synuclein (S7820-500UG), tetrachloroauric acid solution ($HAuCl_4$), ethylenediaminetetraacetic acid (EDTA), 2-imninothiolane hydrochloride, MWCNTs-COOH (thin; extent of labeling: >8% carboxylic acid functionalized; avg. diam. × L 9.5 nm × 1.5 μm), N,N-dimethylformamide (DMF; 99%) and bovine serum albumine (BSA) were purchased form Sigma-Aldrich (Steinheim, Germany). Maleimide PEG amine (Mal-PEG-NH_2; MW 2000 Da) was purchased from Nanocs. Alumina solution (γ-Al_2O_3) 0.3 μm and 0.05 μm were purchased from Gravimeta (Portugal). Eight inches microfiber cloth (Buehler) was used to perform the mechanical cleaning of the working electrode. Ultrapure water (18.2 MΩcm^{-1} resistivity) was produced by a Milli-Q Simplicity 185 system (Millipore, Molsheim, France).

4.2 – Electrochemical Measurements

The voltammetric and impedimetric measurements were realized using an Autolab electrochemical system (Metrohm-Eco Chemie, The Netherlands) equipped with PGSTAT-30 controlled by a computer through the Model NOVA version 1.9 software. The electrochemical cell was mounted using a conventional three-electrode cell, which included a modified pyrolytic graphite electrode basal plane (PGEB; A =7.07 mm^2; ALS Co., Ltd.; Tokyo, Japan) as a working electrode, a Ag|AgCl|3 M KClsat reference electrode to which all potentials are referred and a platinum counter electrode.

CV was performed in a potential range from -0.4 to 0.8 V at scan rate 100 mV s^{-1}. SWV measurements were performed by varying the potential from -0.2 to 0.9 V at 100 mV s^{-1}. The

other used SWV parameters were the frequency of 25 Hz, amplitude of 0.040 V and the step of 0.0040 V. EIS results were obtained using a set potential of 200 mV with an amplitude perturbation of 5 mV and using a frequency range from 10^{-1} to 10^{5} Hz.

The used electroactive indicator for all electrochemical assays was 2.5 mM $K_3[Fe(CN)_6]/K_4[Fe(CN)_6]$ in 0.1 M (pH=7.4) phosphate buffer solution (PBS).

4.3 – Immunosensor Fabrication

Before any modification, the PGE surface was carefully and repetitively cleaned with 0.3 µm and 0.05 µm alumina on a microfiber cloth. Then, the surface was rinsed with ethanol, briefly sonicated and, posteriorly rinsed with Milli-Q water. Finally, the surface of PGE was activated by performing a CV in 0.5 M H_2SO_4 solution in the range of 0 to 1.6 V *vs.* Ag/AgCl/Cl sat. at a scan rate of 100 mV s^{-1}. This activation process was executed several times until typical pyrolite graphite voltammograms were obtained. To finish, the PGE was washed with Milli-Q water and subsequently modified.

4.3.1 – Drop Cast of Multi-walled Carbon Nanotubes

A suspension of MWCNTs was prepared in DMF (1 mg mL^{-1}) and sonicated for 24 h. The immobilization process of MWCNTs was executed by drop-casting on the surface of PGE and set to dry in an infra-red lamp (SICCATHERM; 250 W HG; 240 V E27/ES) for 30 minutes. In order to optimize the amount of MWCNTs to use on the nanocomposite and the optimum amount of the nanocomposite to immobilize on the PGE, six different amounts of the MWCNTs solution were tested, namely, 1.0, 2.0, 3.0, 5.0, 6.0 and 9.0 µL.

4.3.2 – Drop Cast of PEG:MWCNTs

PEG solutions (1 mg mL^{-1} and 0.5 mg mL^{-1}) were prepared in Milli-Q water and stirred until a transparent solution was obtained.

The chemical structure of the Mal-PEG-NH_2 is represented in the figure 13 and its principal characteristics are exposed in the table 2. This specific type of PEG belongs to the heterobifunctional polyethylene glycol crosslinkers group, which is composed by a thiol maleimide group and a reactive primary amine group. The fact of using a PEG with these two crosslinkers (maleimide and amine) makes it easier to use since its solubility in water is improved [95].

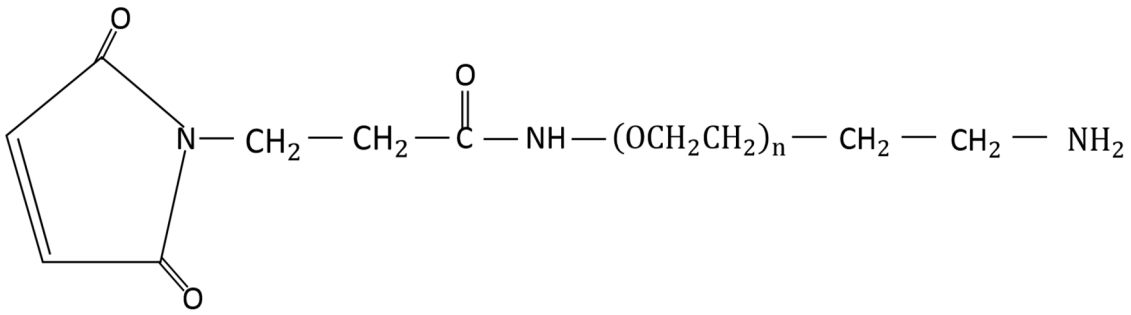

Figure 13 – Chemical structure of maleimide-PEG-amine.

Table 2 – Specifications of Mal-PEG-NH_2.

Composition	Maleimide PEG NH_2
Molecular Weight	2000 Da
Solubility	10 mg mL^{-1}, clear in water, DMSO, chloroform, etc
Appearance	White/off-white semi-solid (varies with the molecular weight
Reactive to	Sulfhydryl, NHS
Reactive Groups	Maleimide and amine

Two different concentrations of PEG (1 and 0.5 mg mL^{-1}) were studied in order to obtain the optimum concentration of PEG to be used in the PEG:MWCNTs:AuNPs nanocomposite production. Two different proportions, 1:10 and 1:1 (v:v), of a PEG:MWCNTs suspension, were tested. For the proportion 1:10, were tested the two solutions of 1 mg mL^{-1} and 0.5 mg mL^{-1} of PEG by drop-casting, on the surface of the electrode, 5 µL of a suspension containing 2 µL of PEG and 20 µL of MWCNTs (1 mg mL^{-1}) and set to dry in an infra-red lamp, for 30 minutes. The same process was repeated for the proportion of 1:1, however, and considering this proportion, the prepared suspension of PEG:MWCNTs was the result of a mixture of 10 µL of PEG (1 and 0.5 mg mL^{-1}) and 10 µL of MWCNTs (1 mg mL^{-1}).

The next step necessary for obtaining a nanocomposite that allows a highly and sensitive detection of α-synuclein is the optimization of the proportions (v:v) of PEG (0.5 mg mL^{-1}):MWCNTs (1 mg mL^{-1}) to use as an indicator to the synthesis of the PEG:MWCNTs:AuNPs nanocomposite, namely, 1:0, 1:1 1:3, 1:5, 1:6, 1:8, 1:10 and 0:1.

4.3.3 – Synthesis of AuNPs

AuNPs were obtained through the standard Turkevich-Method [96]. First, 8.86 µL of 0.5 M $HAuCl_4$ solution were added to 12.5 mL of Milli-Q water and the mixture was refluxed with heat and stirring. When the mixture started to boil, 1.25 mL of trisodium citrate solution (38.8 mM) was added and the final mixture was refluxing for more 15 min. Afterwards, the liquid was extracted and cooled at room temperature.

4.3.4 – PEG:MWCNTs:AuNPs Nanocomposite Preparation

For all the proportions described below, the amount of PEG:MWCNTs:AuNPs nanocomposite immobilized on the PGE surface was 5 µL and the drop-casting technique was used, followed by a drying time of 30 minutes in an infra-red lamp. All the nanocomposite suspensions were prepared immediately before being used.

The process of optimization started by considering two proportions: 1:8 and 1:10 (PEG:MWCNTs; v:v), that were optimized initially, and the following ratios of **PEG:MWCNTs:AuNPs (v:v:v)** were subsequently tested:

- **PEG:MWCNTs:AuNPs 1:8:10 and 1:10:10**
- **PEG:MWCNTs:AuNPs 1:8:20 and 1:10:20**
- **PEG:MWCNTs:AuNPs 1:8:30 and 1:10:30**
- **PEG:MWCNTs:AuNPs 1:8:40 and 1:10:40**
- **PEG:MWCNTs:AuNPs 1:10:50 and 1:10:60**

4.4 – Antibody Immobilization

The antibody was modified through thiolation with Traut's Reagent and EDTA. A mixed solution containing the monoclonal antibody against α-synuclein was prepared in PBS (0,1 M; pH= 7.4), 1 µL of EDTA (0.28 mol L^{-1}) and 82.6 µL of 2-iminothiolane (0.198 mg mL^{-1}). The prepared solution reacted for 50 minutes at room temperature. After the reaction, 389.4 µL of PBS were added to the solution, in order to make up a total volume of 500 µL needed for the next step. Then, the resulting solution was purified by passing it through a sephadex PD Mini-Trap G-25 column (GE Healthcare), following the gravity protocol. 1.0 mL of PBS was added to the column to collect the eluate.

To immobilize the antibody, the PEG:MWCNTs:AuNPs modified electrode was immersed in 170 µL of the prepared antibody solution (5.0, 10.0. 15.0 and 20.0 µg mL^{-1}) and reacted for 2 hours at room temperature, then it was incubated at 4 °C for 12 hours. The modified PGE was thoroughly rinsed with Milli-Q water to remove the unbound antibody and remained in PBS for 1 hour at 4 °C in order to stabilize the immobilization process.

The remaining non-specific binding sites on the electrode surface were blocked with BSA at 4ºC for 20 minutes. The electrodes were further rinsed with Milli-Q water and immersed in PBS solution for 1 hour at 4 °C in order to stabilize the immobilization process. For that purpose, two concentrations of BSA were tested 1.0 and 0.5% (w/v).

4.5 – α-Synuclein Electrochemical Detection

The BSA/Anti-α-syn/[PEG:MWCNTs:AuNPs]/PGE electrode was immersed in 200 µL of α-syn solutions prepared in a PBS solution at pH 7.4 for 50 minutes at RT. Then the electrodes were thoroughly rinsed with Milli-Q water and PBS to remove the unbound antigen. The range of concentrations of α-syn tested in this work was between 500 and 20000 ug mL^{-1}. The parameter used to evaluate the results and to obtain α-syn analytical curves was the current reduction (%IR), that represents the inhibition percentage of the selected antigen concentration and is determined through the subsequent equation 1:

$$\%IR = 1 - \frac{I_p}{I_p^0} \times 100 , \quad (1)$$

where I_p^0 and I_p are the peak currents of $[Fe(CN)_6]^{3-/4-}$ before and after the incubation of the immunosensor with α-syn, respectively.

The detection (LOD) and quantification (LOQ) limits were obtained (equations 2 and 3) using the standard deviation of the intercepts and the average of slopes of the straight lines from the analytical curves, respectively [97].

$$LOD = 3 \times \frac{S_{y/x}}{b} , \quad (2)$$

$$LOQ = 10 \times \frac{S_{y/x}}{b} , \quad (3)$$

where b is the interception of the regression line and Sy/x is the standard deviation in the y-direction.

Chapter 5

Results and Discussion

5.1 - Immunosensor Fabrication

5.1 - Optimization of Multi-walled Carbon Nanotubes

The pyrolytic graphite electrodes are well known for presenting hydrophobic characteristics, which are responsible for stabilizing the MWCNTs films [98]. MWCNTs are known for presenting fast electron transfer kinetics, electrocatalysis features and a large surface area [36], [40], which are particularly relevant for the development of immunosensors.

The total amount of MWCNTs to deposit on the surface of the PGE was optimized by testing six different volumes, namely, 1.0, 2.0, 3.0, 5.0, 6.0 and 9.0 µL (figure 14). Drop casting of 1 µL of MWCNTs at 1 mg/mL onto the PGE surface promoted the major current increase, namely about 2.75 times higher comparatively with the bare PGE, followed by the 5 µL (about 154.33 % increase). All other volumes promoted lower signal increments. Thus, and considering that 1 µL may not be enough for drop-casting of the nanocomposite, 5 µL was selected.

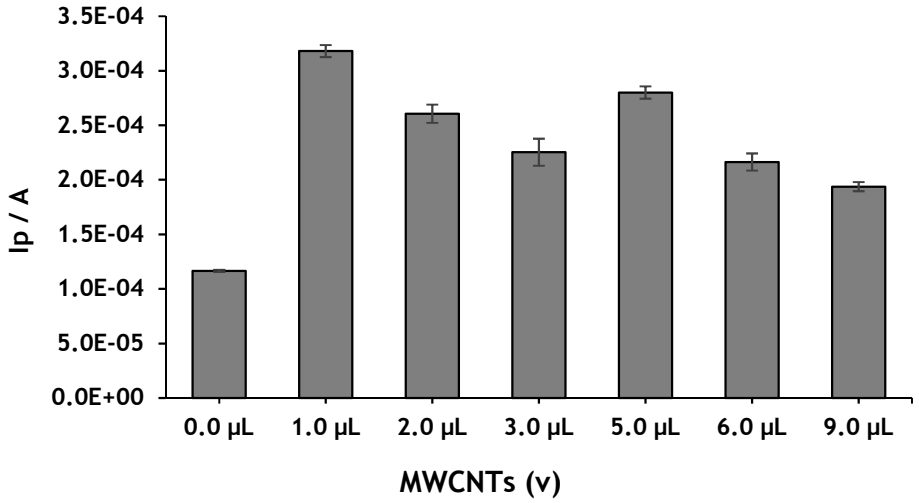

Figure 14 - Effect of the MWCNTs volumes (0.0, 1.0, 2.0, 3.0, 5.0, 6.0 and 9.0 µL) on the peak current of the modified PGE. Experimental conditions: 2.5 mmol L^{-1} $[Fe(CN)_6]^{3-/4-}$ in 0.1 M PBS solution (pH=7.4) at 100 mV s^{-1}.

5.1.2 – Optimization of the PEG concentration and PEG:MWCNTs

Firstly, in this stage, the principal objective was to select the optimum concentration of PEG to further use in the production of PEG:MWCNTs:AuNPs nanocomposite. For this purpose, two concentrations of PEG (0.5 and 1 mg/mL) were tested in the PEG/MWCNTs ratios of 1:1 and 1:10 (v/v) (figure 15). Regarding the PEG concentration, the peak current increased with the lowest of PEG concentration for both ratios. Moreover, the greatest current increase was observed for the PEG:MWCNTs ratio of 1:10 (figure 15 (a) and (b)), for both concentrations of PEG. Thus, 0.5 mg/mL was considered the most favorable concentration of PEG to further use in the synthesis of PEG:MWCNTs:AuNPs nanocomposite.

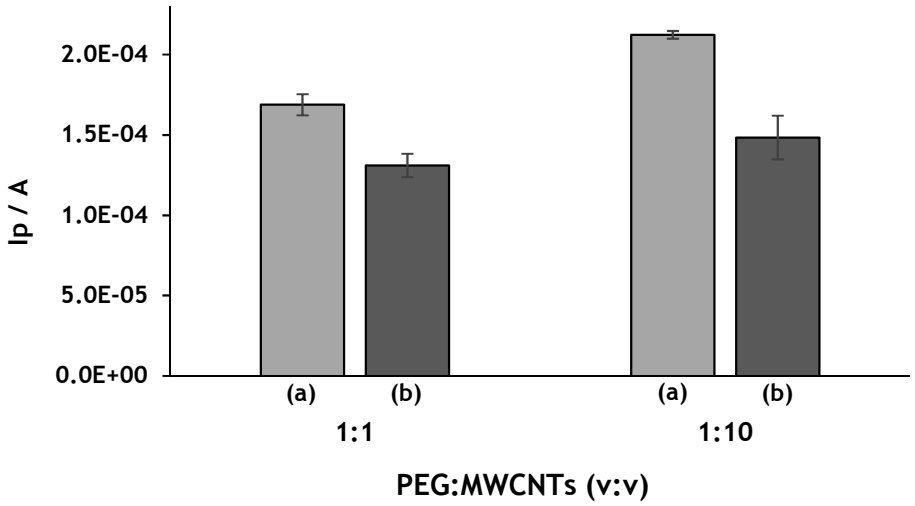

Figure 15 – Influence of the PEG concentration in the PEG:MWCNTs ratios in the current peak using $[Fe(CN)6]^{3-/4-}$ as an electroactive indicator at a concentration of 2.5 mM in 0.1 M PBS solution (pH=7.4). (a): PEG:MWCNTs ratio for the PEG concentration of 0.5 mg/mL and (b): PEG:MWCNTs ratio for the PEG concentration of 1 mg/mL.

Subsequently, in order to optimize the ratio of PEG (0.5 mg mL^{-1}):MWCNTs (1 mg mL^{-1}) (v/v) to further be used in the synthesis of the PEG:MWCNTs:AuNPs nanocomposite, eight different proportions, 1:0, 1:1, 1:3, 1:5, 1:6, 1:8, 1:10 and 0:1 were investigated (figure 16). The ratio 1:0 promoted a minor electrical conductivity as compared to the other modifications due to the specific characteristics of PEG, namely its insulating nature [44]. As expected, the ratio 0:1 was the one that displayed the higher current, which can be explained by the highly conductive properties of MWCNTs [40]. The increase of MWCNTs and simultaneous decrease of PEG in the PEG:MWCNTs nanocomposite originated the higher enhancement of the signal, thus the 1:10 (v/v) PEG:MWCNTs ratio was considered the optimum one. Additionally, these results also showed that MWCNTs contribute more significantly than PEG to the beneficial impact on the current intensity. These results are in accordance to the electrochemical properties of these two compounds [40], [44].

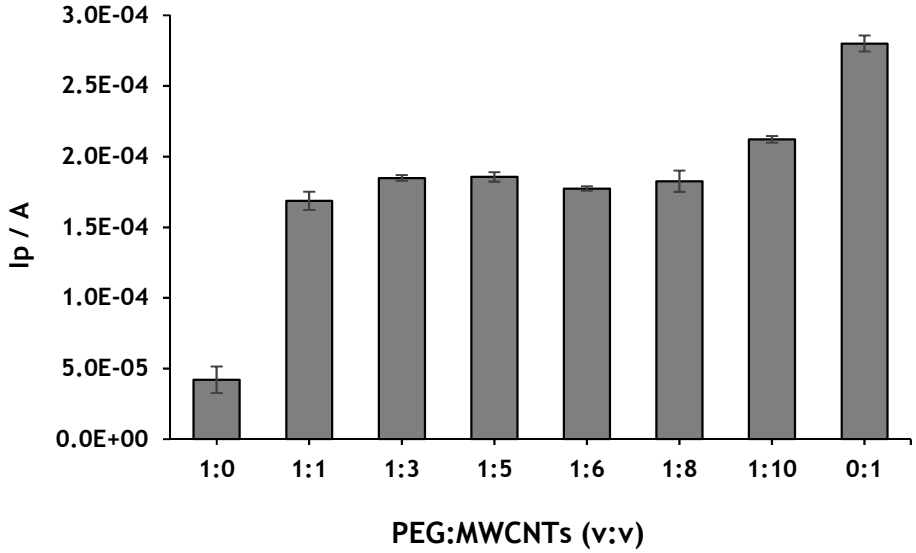

Figure 16 – Effect of the PEG:MWCNTs ratios (1:0, 1:1, 1:3, 1:5, 1:6, 1:8, 1:10 and 0:1, v:v) on the current peak of the modified PGE using $[Fe(CN)6]^{3-/4-}$ as an electroactive indicator at a concentration of 2.5 mM in 0.1 M PBS solution (pH=7.4) at 100 mV s^{-1}.

5.1.3 – Optimization of PEG:MWCNTs:AuNPs Nanocomposite

First and, in order to better understand the behavior of AuNPs and the amount necessary for a proper immobilization in the electrode surface, were tested six different proportions of PEG:AuNPs (v:v), namely 1:0, 1:3, 1:10, 1:20, 1:30 and 0:1. Analyzing the effect of these two species was clear that AuNPs produced a higher current intensity when compared with PEG. These results are in accordance with their properties, namely, the electronic and biocompatible characteristics of AuNPs [32] and the insulating effect of PEG [44]. On the other hand, these results also demonstrated that it is necessary to increase the proportion of AuNPs in the PEG:MWCNTs:AuNPs nanocomposite to achieve a higher current intensity and, consequently, a highly selective and sensitive detection (figure 17).

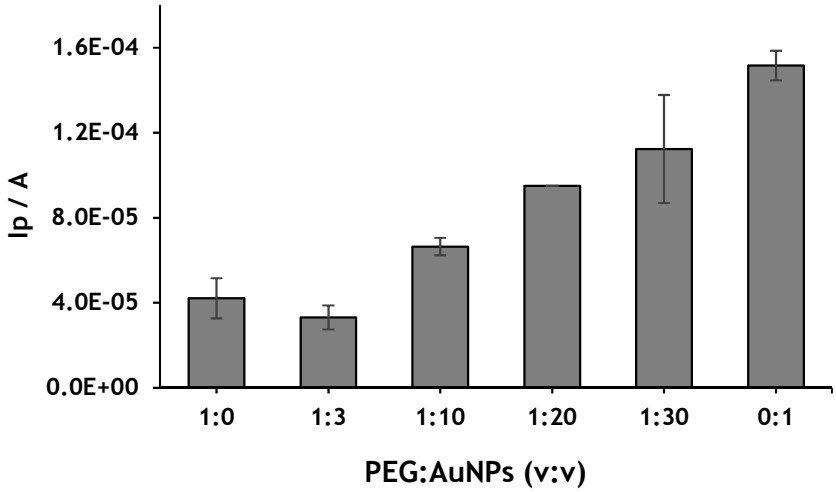

Figure 17 – Influence of the tested PEG:AuNPs proportions (1:0, 1:3, 1:10, 1:20, 1:30 and 0:1, v:v) on the current peak of the modified PGE using $[Fe(CN)6]^{3-/4-}$ as an electroactive indicator at a concentration of 2.5 mM in 0.1 M PBS solution (pH=7.4) at 100 mV s^{-1}.

Considering the previously optimum proportion of 1:10 (PEG:MWCNTs; v:v), seven different proportions (1:10:0, 1:10:10, 1:10:20, 1:10:30, 1:10:40, 1:10:50 and 1:0:10 (v:v:v)) were tested regarding the incorporation of the AuNPs into the nanocomposite (figure 18). The introduction of AuNPs allowed to achieve a higher sensitivity, when compared with the PGE modification with just two components ([PEG:MWCNTs]/PGE), for all the proportions tested, except for the proportions 1:10:10 (figure 18). Since the 1:10:40 (v:v:v) PEG:MWCNTs:AuNPs ratio promoted the best signal (196.7% higher current for [PEG:MWCNTs:AuNPs]/PGE than PGE) , it was considered the optimum one. Moreover, it was possible to verify that MWCNTs contributed more significantly than AuNPs to the enhancement of the current intensity, which could indicate that MWCNTs led to a greater increase in active surface area than AuNPs.

CV, SWV and EIS were used in order to characterize the impact of each modification involved in the fabrication of the nanocomposite and thus to optimize its construction. All the assays were obtained in 2.5 mM $[Fe(CN)6]^{3-/4-}$ solution as an electroactive indicator in 0.1 M PBS solution (pH=7.4). Figure 19 presents the representative cyclic voltammograms (figure 19 (A)), the square wave voltammetric response (figure 19 (B)) and the impedance spectra as Nyquist plots (figure 19 (C) and (D)) of the bare-PGE, MWCNTs/PGE, PEG/PGE, [PEG:MWCNTs]/PGE and [PEG:MWCNTs:AuNPs]/PGE.

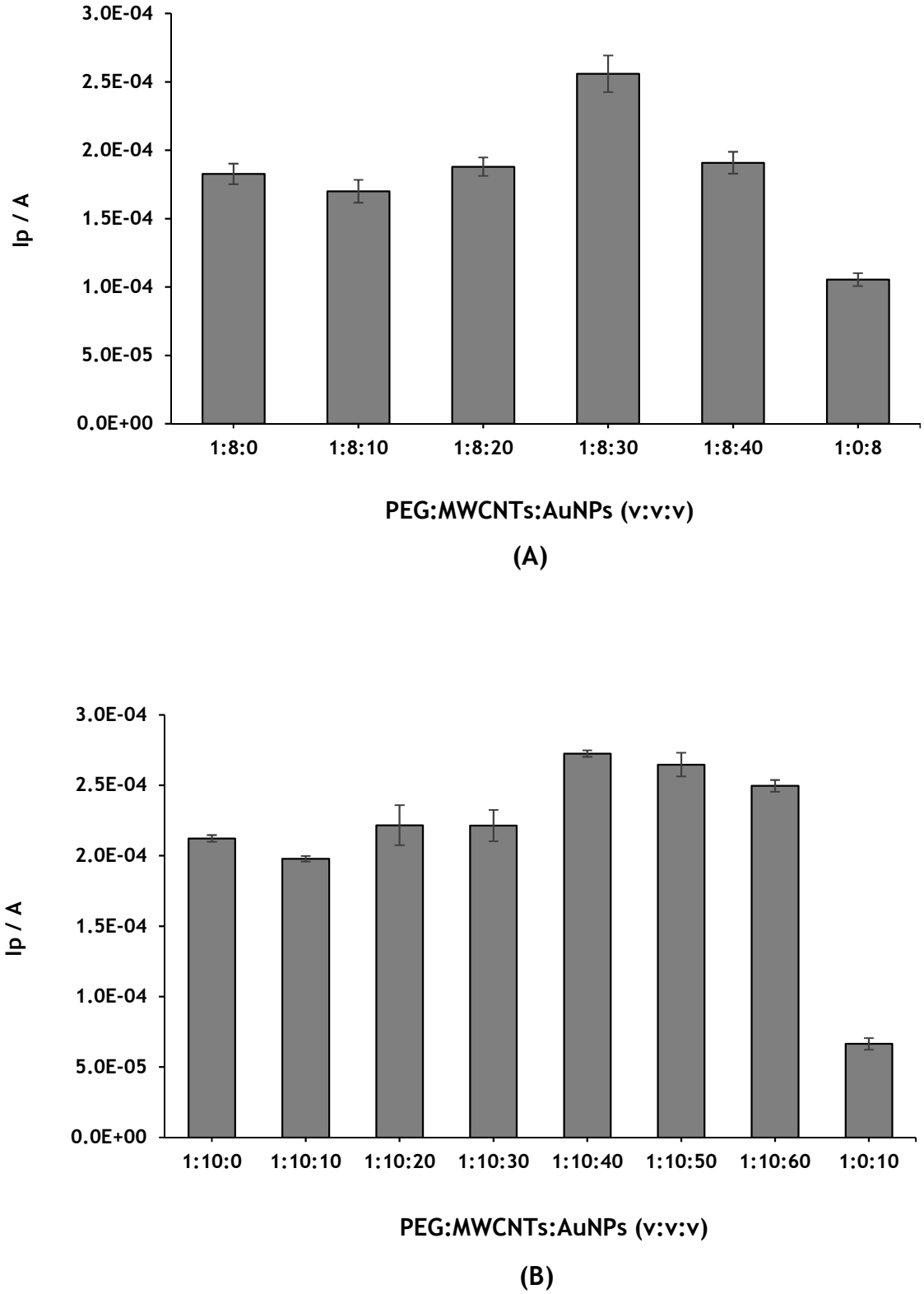

Figure 18 - Optimization of the PEG:MWCNTs:AuNPs ratio: **(A)** Effect of the PEG:MWCNTs:AuNPs ratio (1:8:0, 1:8:10, 1:8:20, 1:8:30, 1:8:40 and 1:0:8, v:v:v) on the peak current of the modified PGE. **(B)** Effect of the PEG:MWCNTs:AuNPs ratio (1:10:0, 1:10:10, 1:10:20, 1:10:30, 1:10:40, 1:10:50, 1:10:60 and 1:0:10, v:v:v) on the peak current of the modified PGE. Experimental conditions: 2.5 mmol L^{-1} $[Fe(CN)_6]^{3-/4-}$ in 0.1 M PBS solution (pH=7.4) at 100 mV s^{-1}.

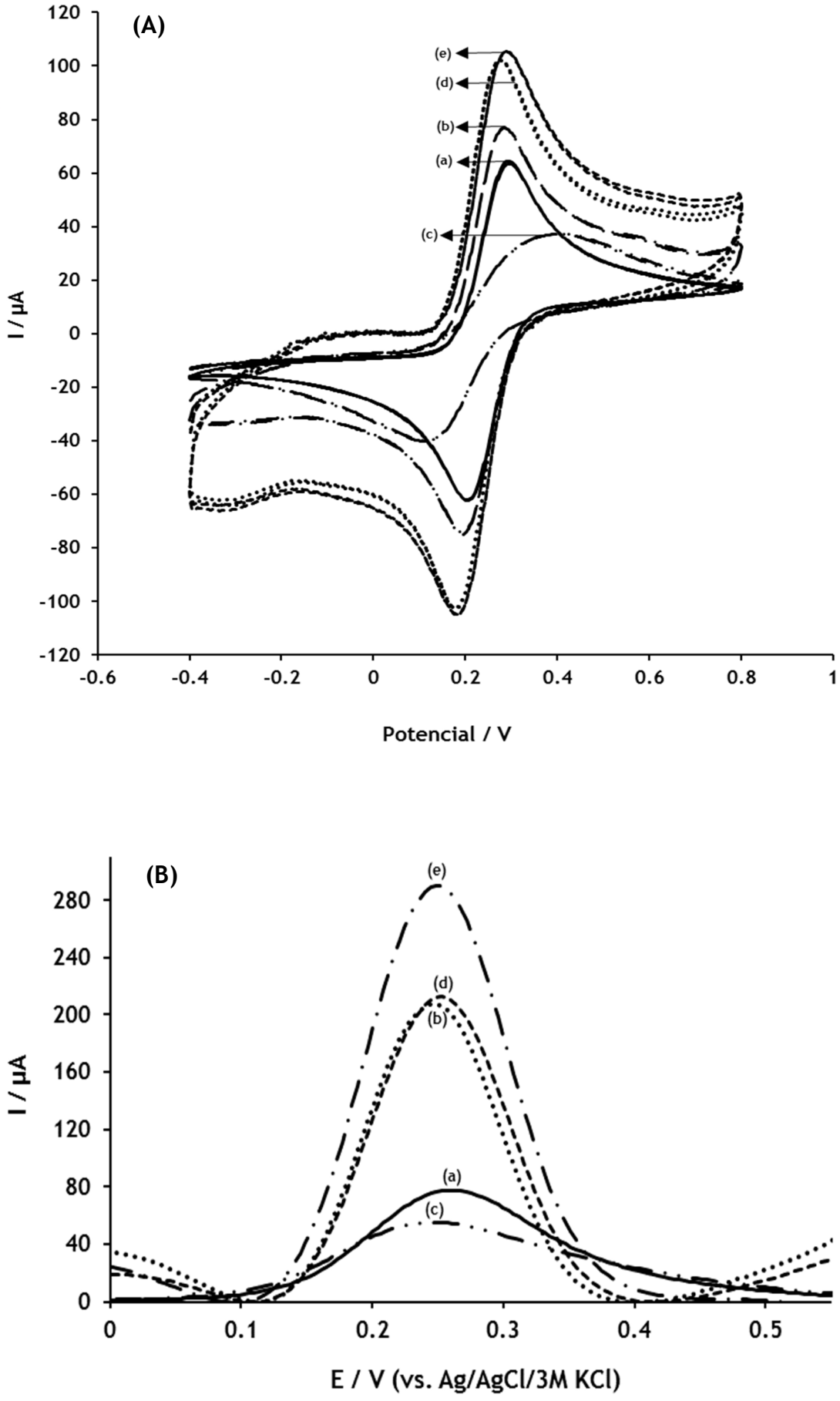

Figure 19 (continued on the next page, legend follows).

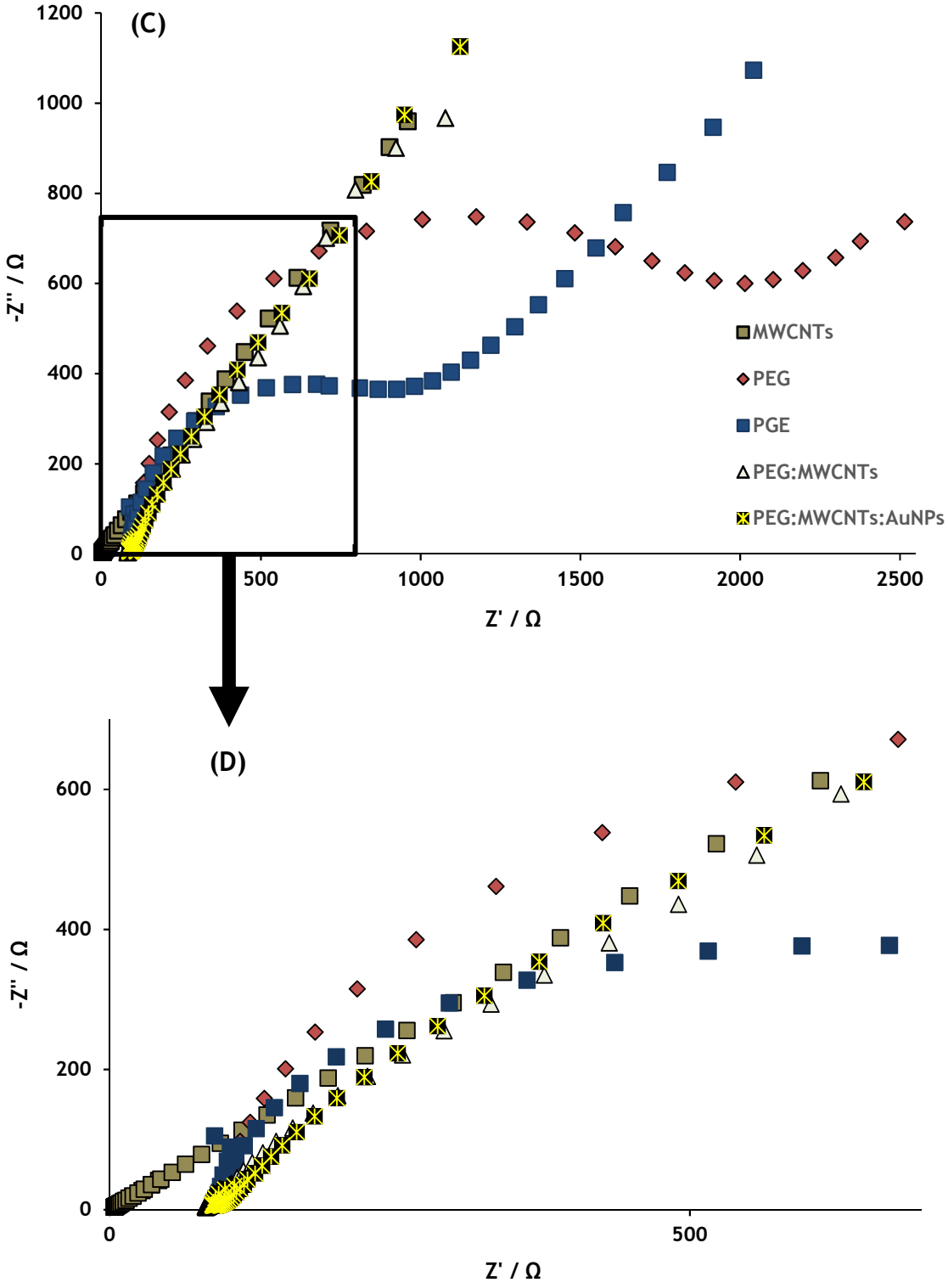

Figure 19 - **(A)** CV voltammograms of the (a) bare-PGE, (b) MWCNTs/PGE, (c) PEG/PGE, (d) [PEG:MWCNTs]/PGE ratio (v:v) of 1:10 and (e) [PEG:MWCNTs:AuNPs]/PGE ratio (v:v:v) of 1:10:40 in 2.5 mM $[Fe(CN)_6]^{3-/4-}$ solution in 0.1 M PBS solution (pH=7.4) at 100 mV s^{-1}; **(B)** SW voltammograms of (a) bare-PGE, (b) MWCNTs/PGE, (c) PEG/PGE, (d) [PEG:MWCNTs]/PGE ratio (v:v) of 1:10 and (e) [PEG:MWCNTs:AuNPs]/PGE ratio (v:v:v) of 1:10:40 obtained in 2.5 mM $[Fe(CN)_6]^{3-/4-}$ solution in 0.1 M PBS solution (pH=7.4) with a frequency of 25 Hz, amplitude of 40 mV and step potential of 4 mV; **(C)** Nyquist plots of (a) bare-PGE, (b) MWCNTs/PGE, (c) PEG/PGE, (d) [PEG:MWCNTs]/PGE ratio (v:v) of 1:10 and (e) [PEG:MWCNTs:AuNPs]/PGE ratio (v:v:v) of 1:10:40 performed in 2.5 mM $[Fe(CN)_6]^{3-/4-}$ solution in 0.1 M PBS

solution (pH=7.4) applying a frequency range from 10^{-1} to 10^{5} Hz with an amplitude perturbation of 5 mV and 0.2 V of conditioning potential; **(D)** displays in more detailed the semicircle portion of all Nyquist plots presented in figure 20 (**C**).

The bare-PGE surface exhibited well-defined and characteristic cathodic and anodic peaks corresponding to the reduction and oxidation, respectively, of the $[Fe(CN)6]^{3-/4-}$ redox couple (figure 19, curve (a)). The MWCNTs modified PGE exhibited a higher conductivity when compared to the bare-PGE (figure 19, curve (b)), which can be explained by the highly conductive properties of MWCNTs and high electroactive surface area [36]. As expected, the modification with PEG only presented the lowest current (figure 19, curve (c)). However, when PEG and MWCNTs were combined in a nanocomposite, a significant current increase (65.9% higher current for [PEG:MWCNTs]/PGE than PGE) was observed (figure 19, curve (d)). The peak current increased, even more, when PGE was modified with the PEG:MWCNTs:AuNPs nanocomposite (figure 19 (A), curve (e)) due to the synergetic effects between the three components. In addition, this pattern of variation is in accordance with the results achieved by SWV (figure 19 (B)) and EIS (figure 19 (C-D)). Impedance spectra are characterized by possessing a semicircle portion and a linear portion, which can be used to describe the interface properties of the PGE for each modification step: MWCNTs/PGE, PEG/PGE, [PEG:MWCNTs]/PGE and [PEG:MWCNTs:AuNPs]/PGE (figure 19 (C) and (D)). The redox process at the bare PGE displayed low resistance (568.3 Ω) as previously reported [99]. With the drop-casting of MWCNTs, no semicircle can be detected, demonstrating that the interfacial electron transfer resistance was improved due to their inherent properties. The adsorption of PEG:MWCNTs onto the PGE electrode lead to a significant decrease in the resistance value (137.4 Ω), when compared with the PEG-PGE (2248 Ω). The last change in the Nyquist plot observed in the fabrication process of the [PEG:MWCNTs:AuNPs]/PGE was characterized for the absence of a significant semicircle, indicating that the interfacial electron transfer resistance was improved due to the addition of AuNPs to the [PEG:MWCNTs]/PGE. This phenomenon can be explained by the fact of AuNPs present a large specific surface area and high conductivity, that when mixed with MWCNTs and PEG display synergetic effects.

5.1.4 – Antibody Immobilization onto the [PEG:MWCNTs:AuNPs]/PGE

The antibodies were functionalized through a chemical modification to create thiol groups in the Fc fragment and to offer a greater number of paratopes available for recognition of the target. The principal objective of this process is to promote stability, proper orientation, and the binding of the antibody to the PEG:MWCNTs:AuNPs nanocomposite. The specific type of PEG used in the nanocomposite development is composed by a thiol maleimide group and a reactive primary amine group that are responsible for helping in the antibody immobilization and thus providing stability to the antibody. The maleimide group is responsible for readily reacting with thiol groups at a pH between 6.5 and 7.5 and for allowing the formation of stable thioether bonds, while the amine group has the ability of reacting with NHS, carboxyl and many other specific groups [95].

The two reagents involved in thiolation are EDTA and 2-iminothiolane that are responsible for stopping completely metal sulfhydryl residues and for reacting with the amine groups in the Ab to result in permanent modifications containing terminal sulfhydryl residues [100].

Four different antibody concentrations (5.0, 10.0, 15.0 and 20.0 μg mL^{-1}) were tested in order to immobilize them on the [PEG:MWCNTs:AuNPs]/PG modified electrode and the corresponding percentage of their peak reductions are demonstrated in figure 20.

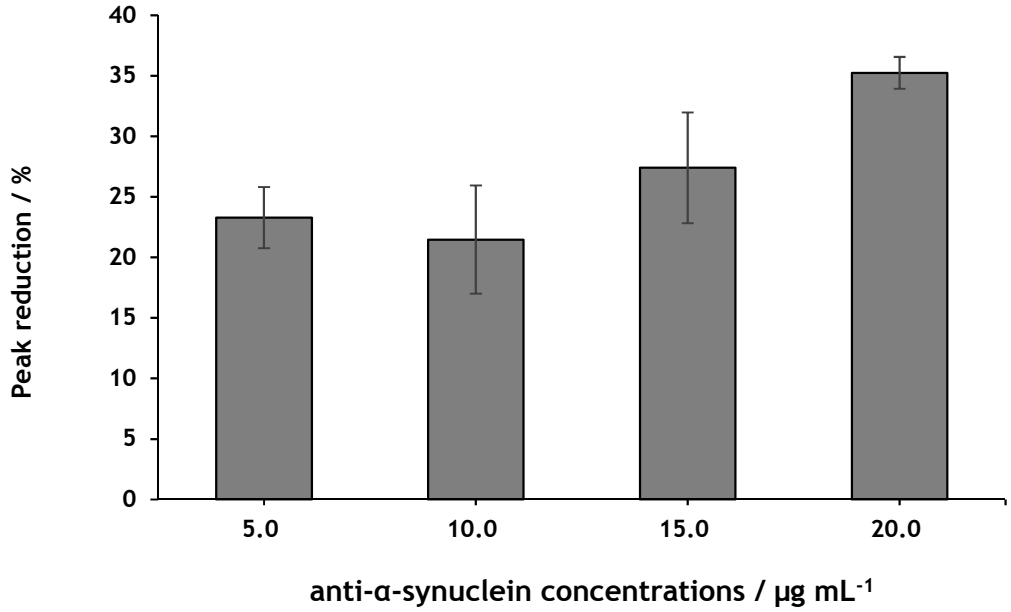

Figure 20 - Influence of the tested antibody concentrations (5.0, 10.0, 15.0 and 20.0 µg mL^{-1}) in the current peak reduction using $[Fe(CN)6]^{3-/4-}$ as an electroactive indicator at a concentration of 2.5 mM in 0.1 M PBS solution (pH=7.4) at 100 mV s^{-1}.

For all the concentrations tested, the antibody immobilization led to a current signal reduction of the $[Fe(CN)6]^{3-/4-}$ redox couple varying from 21 to 35% due to the formation of a protein layer that partially blocked the modified electrode surface. For the three higher concentrations tested (10.0, 15.0 and 20.0 µg mL^{-1}), the signal reduction was proportional to the increase of anti-α-syn concentration being maximal at 20.0 µg mL^{-1}. A representative SWV voltammogram obtained with the immunosensor prepared with 20.0 µg mL^{-1} of anti-α-syn is exhibited in figure 21.

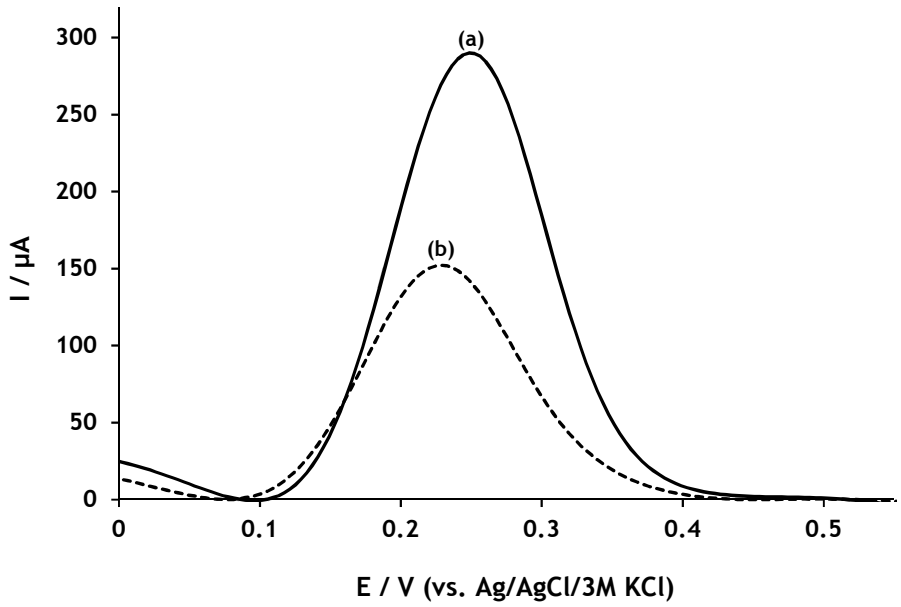

Figure 21 - Representative SW voltammograms of (a) [PEG:MWCNTs:AuNPs]/PG modified electrode; (b) anti-α-syn/[PEG:MWCNTs:AuNPs]/PG modified electrode. Experimental conditions: 2.5 mM $[Fe(CN)6]^{3-/4-}$ as an electroactive indicator in 0.1 M PBS solution (pH=7.4) at 100 mV s^{-1}. Antibody concentration of 20.0 µg mL^{-1}.

BSA was then immobilized onto the surface of the anti-α-syn/[PEG:MWCNTs:AuNPs]/PGE to prevent non-specific binding and to minimize the background signal. Two BSA concentrations were tested, i.e. 0.5 and 1.0 wt% (figure 22).

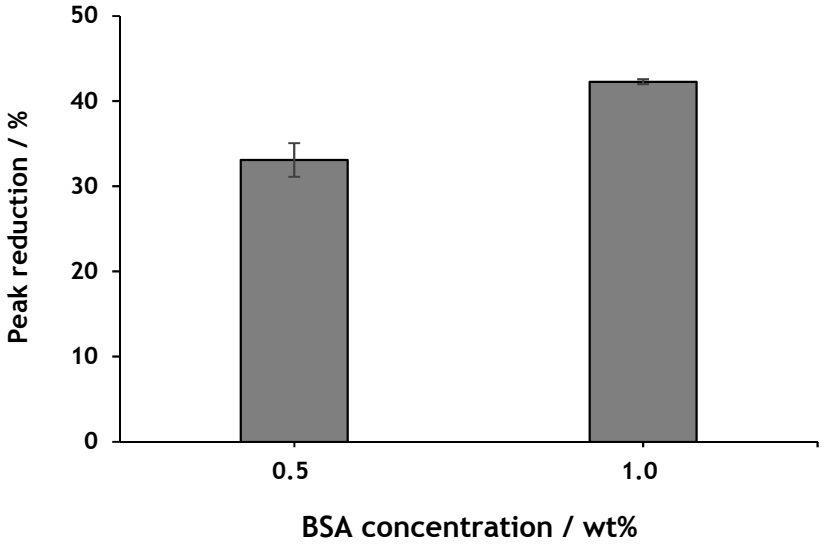

Figure 22 – Influence of the tested BSA concentrations (0.5 and 1.0 wt%) in the current peak reduction using $[Fe(CN)_6]^{3-/4-}$ as an electroactive indicator at a concentration of 2.5 mM in 0.1 M PBS solution (pH=7.4) at 100 mV s^{-1}.

For the two concentrations tested, the signal reduction was proportional to the increase of BSA concentration. 1.0 wt% led to a higher peak reduction, and consequently, to a more efficient blocking process, thus this concentration was considered the optimum one. The SWV response of the immunosensor with the optimum concentration is displayed in figure 23.

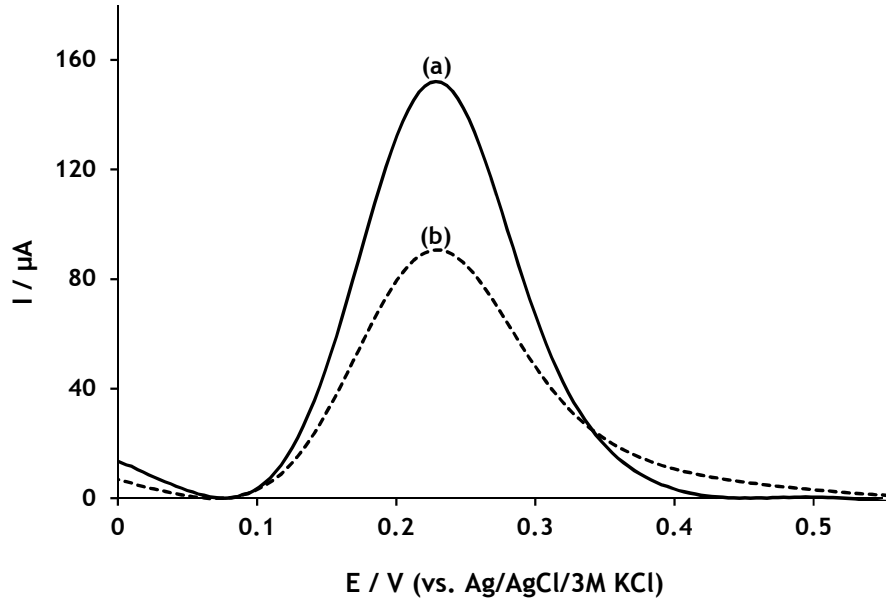

Figure 23 – Representative SW voltammograms of (a) anti-α-syn/[PEG:MWCNTs]/PGE; (b) BSA (1.0 wt%)/anti-α-syn/[PEG:MWCNTs:AuNPs]/PGE. Experimental conditions: 2.5 mM $[Fe(CN)6]^{3-/4-}$ as an electroactive indicator in 0.1 M PBS solution (pH=7.4) at 100 mV s^{-1}.

5.1.5 – Detection of α-synuclein and Electroanalytical Performance of the Immunosensor

The various steps applied in the immunosensor development are illustrated in figure 24.

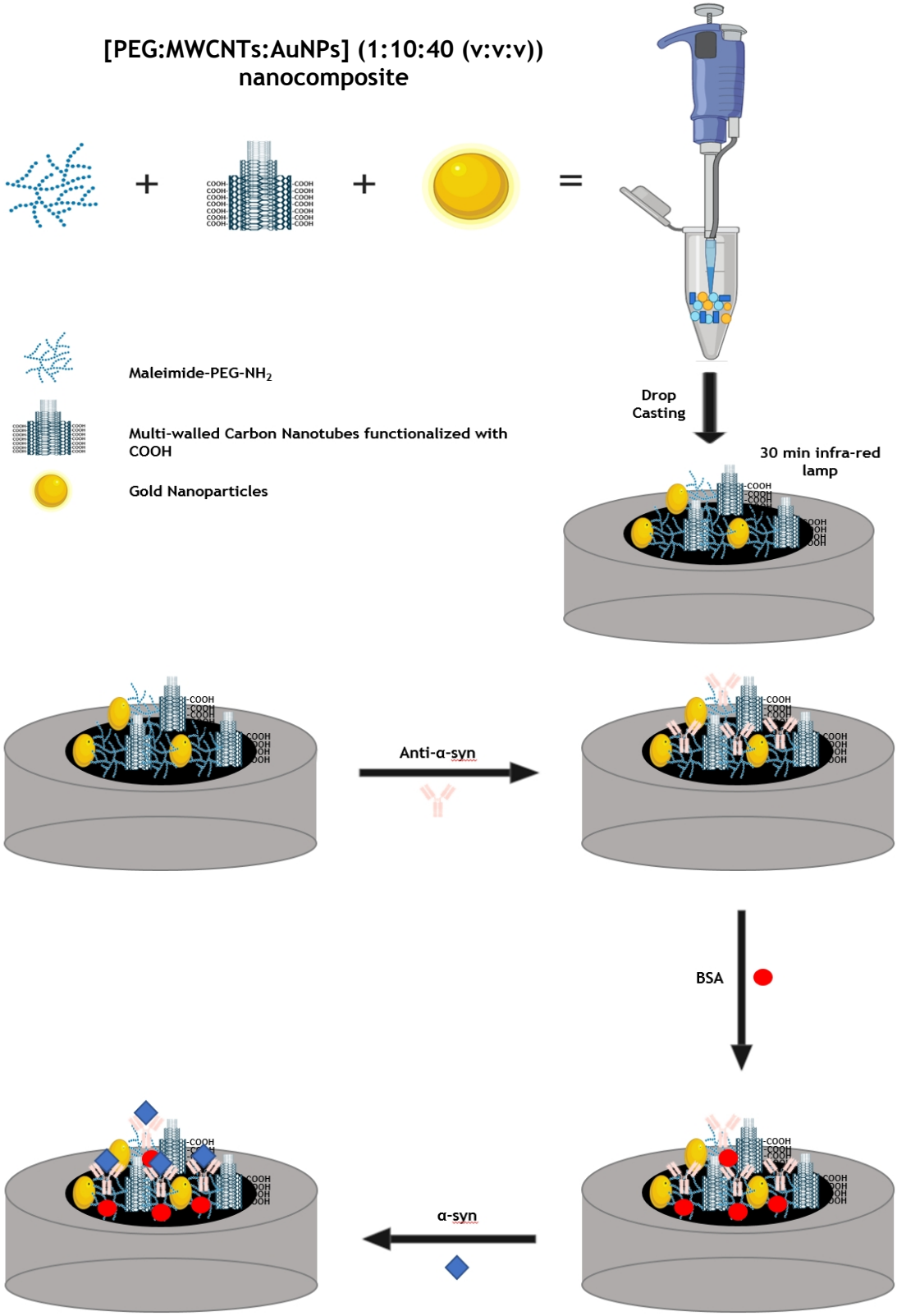

Figure 24 - Representation of the immunosensor fabrication including the nanocomposite preparation.

Figure 25 presents the representative cyclic voltammograms (figure 25 (A)), the square wave voltammetric response (figure 25 (B)) and the impedance spectra as Nyquist plots (figure 25 (C) and (D)) of the bare-PGE, [PEG:MWCNTs:AuNPs]/PGE, anti-α-syn/[PEG:MWCNTs:AuNPs]/PGE, BSA/anti-α-syn/[PEG:MWCNTs:AuNPs]/PGE and α-syn/BSA/anti-α-syn/[PEG:MWCNTs:AuNPs]/PGE. Significant changes in the impedance spectra can be observed after each modification of the pyrolytic graphite electrode with PEG:MWCNTs:AuNPs nanocomposite, anti-α-syn, BSA and α-syn (figure 25 (C) and (D)). The adsorption of PEG:MWCNTs:AuNPs onto the PGE increased the immunosensor surface area and electrical conductivity, consequently, the electron transfer resistance significantly decreased, as indicated by the almost absence of a semicircle. The large surface area, excellent conductivity and strong adsorption ability of AuNPs and MWCNTs improved the electron transfer rate and, thus amplified the electrochemical signal (figure 25 (C) and (D)) [32], [36]. In contrast, after the immobilization of anti-α-syn and BSA, the electron transfer resistance significantly increased (937.9 and 1303.7 Ω, respectively), due to the generation of an insulating protein layer on the [PEG:MWCNTs:AuNPs]/PGE surface. These results also proved that anti-α-syn and BSA were properly immobilized on the [PEG:MWCNTs:AuNPs]/PGE surface. In addition, when the biosensor was exposed to α-syn, a further increase in the electron transfer resistance (2058 Ω) was detected. These results confirmed the successful binding of the antigen to the antibody, with consequent formation of the immunocomplex. The observed changes in the EIS profiles (figure 25 (C) and (D)) are in general in agreement with those exhibited by the cyclic voltammograms (figure 25 (A)) and by the SW voltammograms (figure 25 (B)).

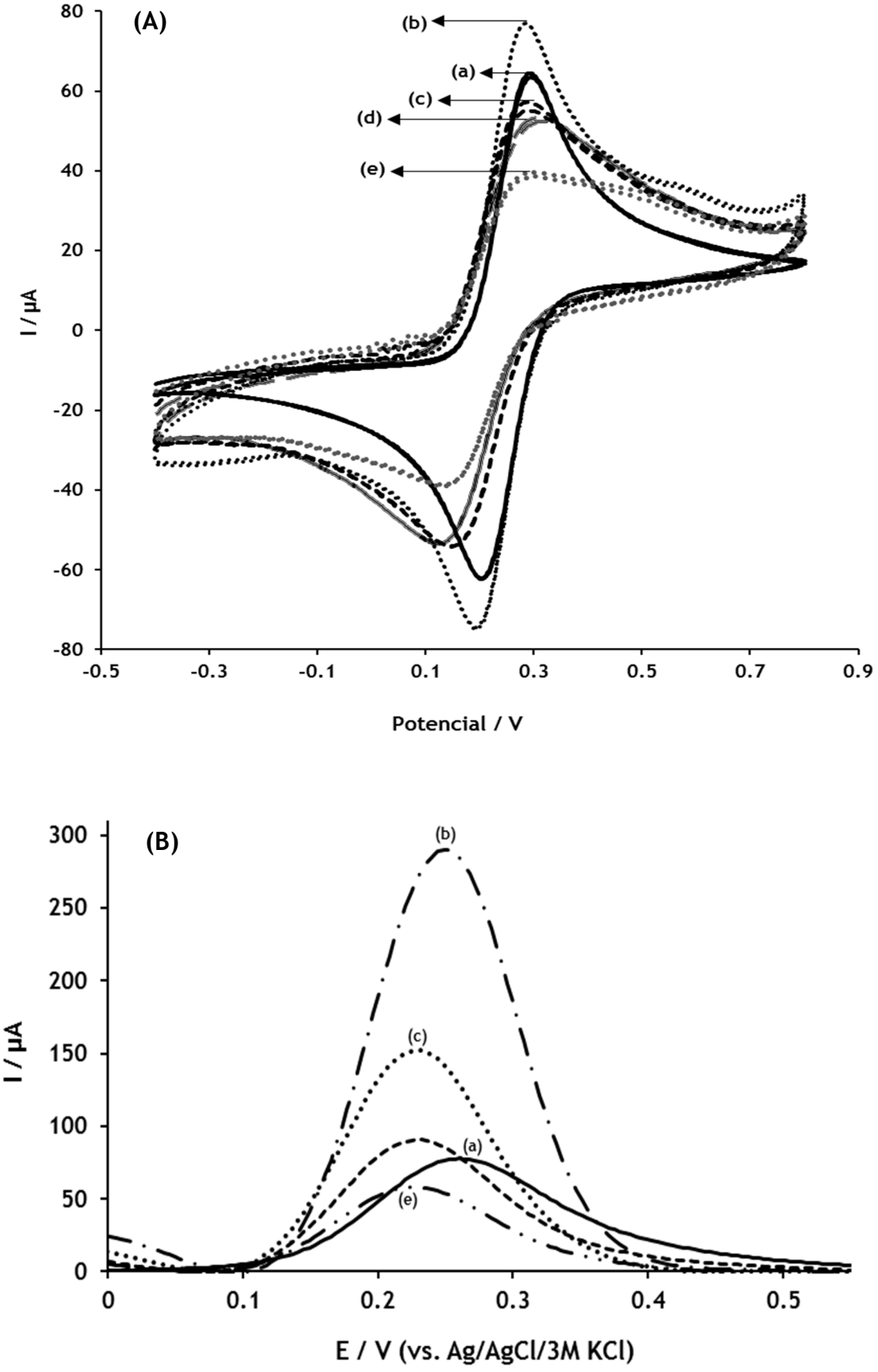

Figure 25 (continued on the next page, legend follows).

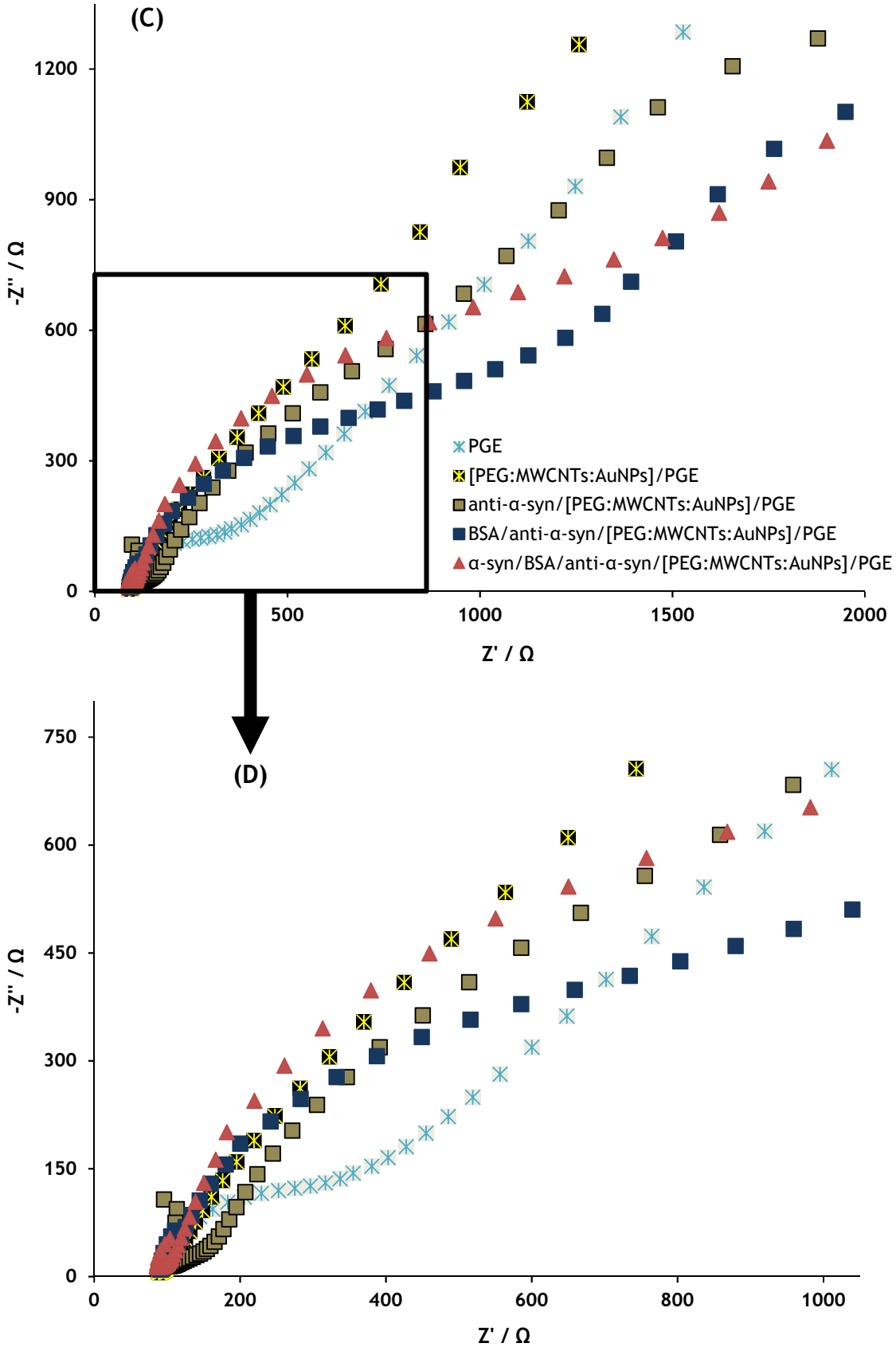

Figure 25 - **(A)** CV voltammograms of the (a) bare-PGE, (b) [PEG:MWCNTs:AuNPs]/PGE ratio (v:v:v) of 1:10:40, (c) anti-α-syn (20μg mL^{-1})/[PEG:MWCNTs:AuNPs]/PGE, (d) BSA (1.0 wt%)/anti-α-syn/[PEG:MWCNTs:AuNPs]/PGE and (e) α-syn(10000 ng mL^{-1})/BSA/anti-α-syn/[PEG:MWCNTs:AuNPs]/PGE

in 2.5 mM $[Fe(CN)_6]^{3-/4-}$ solution in 0.1 M PBS solution (pH=7.4) at 100 mV s^{-1}; **(B)** SW voltammograms of (a) bare-PGE, (b) [PEG:MWCNTs:AuNPs]/PGE ratio (v:v:v) of 1:10:40, (c) anti-α-syn (20μg mL^{-1})/[PEG:MWCNTs:AuNPs]/PGE, (d) BSA (1.0 wt%)/anti-α-syn/[PEG:MWCNTs:AuNPs]/PGE and (e) α-syn(10000 ng mL^{-1})/BSA/anti-α-syn/[PEG:MWCNTs:AuNPs]/PGE obtained in 2.5 mM $[Fe(CN)_6]^{3-/4-}$ solution in 0.1 M PBS solution (pH=7.4) with a frequency of 25 Hz, amplitude of 40 mV and step potential of 4 mV; **(C)** Nyquist plots of (a) bare-PGE, (b) [PEG:MWCNTs:AuNPs]/PGE ratio (v:v:v) of 1:10:40, (c) anti-α-syn (20 μg mL^{-1})/[PEG:MWCNTs:AuNPs]/PGE, (d) BSA (1.0 wt%)/anti-α-syn/[PEG:MWCNTs:AuNPs]/PGE and (e) α-syn (10000 ng mL^{-1})/BSA/anti-α-syn/[PEG:MWCNTs:AuNPs]/PGE performed in 2.5 mM $[Fe(CN)_6]^{3-/4-}$ solution in 0.1 M PBS solution (pH=7.4) applying a frequency range from 10^{-1} to 10^5 Hz with an amplitude perturbation of 5 mV and 0.2 V of conditioning potential; **(D)** Inset displaying the semicircle portions of the Nyquist plots presented in figure 25 (**C**).

Representative voltammograms of the immunosensor response to different concentrations of α-syn (500 – 10000 ng mL^{-1}) are represented in figure 26 (A). As the concentration of α-syn increased, the peak current reduction augmented accordingly, as the result of the formation of the immunocomplex on the PGE surface. The obtained analytical curve (figure 26 (B)), presented good sensitivity (15.2%$_{reduction}$ mL ng^{-1}), good distribution of the data with acceptable quadratic correlation coefficient of 0.99. The LOD and LOQ were established, using equations (2) and (3), to be 8.5 and 1231 ng mL^{-1}, respectively.

The attained immunosensor, in comparison with the previously reported ones for the detection of α-syn, is simpler and faster to fabricate (table 1) [78]–[82]. Moreover, its label free detection obviates the need of expensive enzyme-linked antibody and biotin. However, the attained LOD is higher than the previously reported ones, which can be explained by the fact that no second labeled antibody was applied. Still, due to its simplicity and short analysis time (50 minutes), this immunosensor can be applied in a daily basis as a monitoring device. Still, further optimizations are needed in order to improve the analytical performance of the proposed immunosensor and, also, this immunosensor should be implemented in samples such as serum, blood and cerebrospinal fluid.

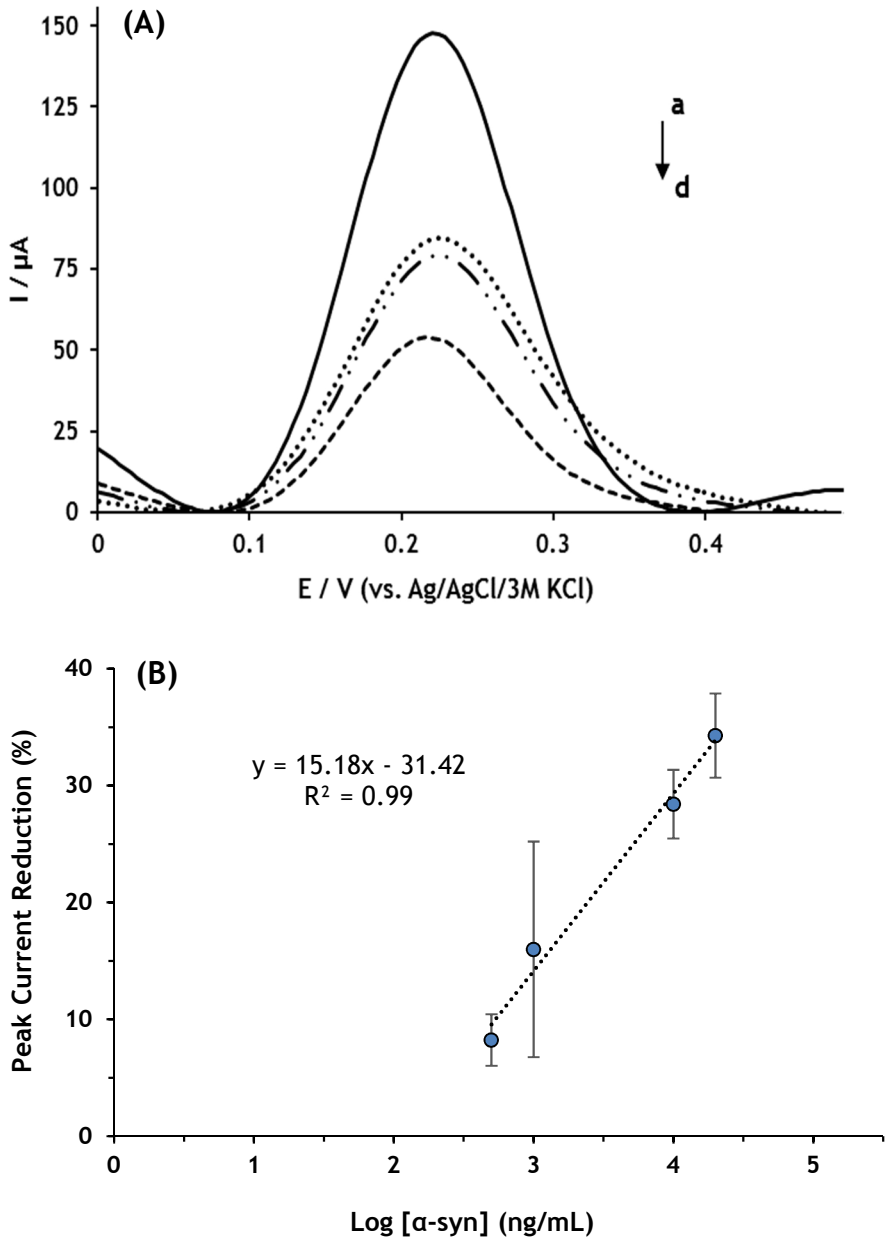

Figure 26 – (A) Representative SW voltammograms of the immunosensor exposed to different concentrations of α-syn (from a to d: 0, 500, 1000 and 10000 ng mL^{-1}). Experimental conditions: 2.5 mM $[Fe(CN)6]^{3-/4-}$ as an electroactive indicator in 0.1 M PBS solution (pH=7.4) at 100 mV s^{-1}. **(B))** Calibration curve for 500 to 20000 ng mL^{-1} based on the obtained current reduction.

Chapter 6

Conclusions and Future Directions

The antemortem diagnosis of PD depends on clinical symptoms and is associated with highly variable specificity and sensitivity. On the other hand, there are still no biomarkers capable of effectively identifying this neurodegenerative disease. Analyzing all these difficulties, the development of immunosensors, capable of detecting earlier this pathology, is a great challenge and, consequently, a great achievement.

In this work, the development of an α-syn-immunosensor that employed the benefits of a PEG:MWCNTs:AuNPs nanocomposite for the detection of α-syn was demonstrated. Electrochemistry, as well as some of the techniques associated with it, constituted a valuable tool in the characterization and analysis of the requisites needed for the construction of the developed immunosensor. The nanostructures were responsible for increasing the sensitivity, selectivity, and performance of the biosensor. They were responsible for creating a suitable microenvironment for proteins immobilization and for improving the electron transfer, which allowed achieving a higher analytical performance.

The first step of the immunosensor development began with the optimization of the PEG:MWCNTs:AuNPs nanocomposite with high electronic conductivity and surface area in order to form an immobilization matrix for further antibody immobilization. The large surface area and the excellent electric conductivity of MWCNTs and AuNPs, together with the specificities of MAL-PEG-NH_2 provided a stable platform for the immobilization of the anti-α-syn. Synergetic effects were achieved between AuNPs and MWCNTs. The antibody was further immobilized on the nanocomposite surface by chemical modification (thiolation) in order to promote proper orientation and a successful immobilization. The label-free detection of α-syn was carried out by determining the percentage of current reduction on the redox pair $Fe(CN)_6^{3-/4-}$ caused by the immunocomplex formation. Thus, the label-free detection presented in this work offers interesting possibilities for detection and monitorization of the selected biomarker, with relatively inexpensive instrumentation. However, nowadays with the limited ability to diagnose PD with only one biomarker, the development of a biosensor able to detect with higher specificity and sensibility and, at the same time, different biomarkers of PD, will be able to improve the diagnostic accuracy of this impairing disease. Also, as future work, the performance and sensitivity of the developed immunosensor should be improved. Moreover, studies of reproducibility, stability and reusability should be fully characterized in order to allow real sample analysis.

References

[1] S. von Campenhausen *et al.*, “Prevalence and incidence of Parkinson’s disease in Europe,” *Eur. Neuropsychopharmacol.*, vol. 15, no. 4, pp. 473–490, Aug. 2005.

[2] M. Shi *et al.*, “Significance and confounders of peripheral DJ-1 and alpha-synuclein in Parkinson’s disease,” *Neurosci. Lett.*, vol. 480, no. 1, pp. 78–82, Aug. 2010.

[3] F. S. Felix and L. Angnes, “Electrochemical immunosensors – A powerful tool for analytical applications,” *Biosens. Bioelectron.*, vol. 102, pp. 470–478, Apr. 2018.

[4] W. Poewe *et al.*, “Parkinson disease,” *Nat. Rev. Dis. Prim.*, vol. 3, p. 17013, Mar. 2017.

[5] S. K. Van Den Eeden *et al.*, “Incidence of Parkinson’s disease: variation by age, gender, and race/ethnicity.,” *Am. J. Epidemiol.*, vol. 157, no. 11, pp. 1015–22, Jun. 2003.

[6] D. W. Dickson *et al.*, “Neuropathological assessment of Parkinson’s disease: refining the diagnostic criteria,” *Lancet Neurol.*, vol. 8, no. 12, pp. 1150–1157, Dec. 2009.

[7] E. Luo, L. Jiao, G. Shen, X.-M. Wu, Q. Xu, and L. Lu, “[Effects of the PEMFs of different intensity on BMD and biomechanical properties of rabbits’ femur].,” *Sheng Wu Yi Xue Gong Cheng Xue Za Zhi*, vol. 22, no. 6, pp. 1168–70, Dec. 2005.

[8] J. S. Sidwell and G. A. Rechnitz, “‘Bananatrode’ - an Electrochemical Biosensor for Dopamine,” *Biotechnol. Lett.*, vol. 7, no. 6, pp. 419–422, 1985.

[9] D. Iacono *et al.*, “Parkinson disease and incidental Lewy body disease: Just a question of time?,” *Neurology*, vol. 85, no. 19, pp. 1670–1679, Nov. 2015.

[10] H.-M. Gao, P. T. Kotzbauer, K. Uryu, S. Leight, J. Q. Trojanowski, and V. M.-Y. Lee, “Neuroinflammation and Oxidation/Nitration of -Synuclein Linked to Dopaminergic Neurodegeneration,” *J. Neurosci.*, vol. 28, no. 30, pp. 7687–7698, Jul. 2008.

[11] M. R. Cookson, “Evolution of Neurodegeneration,” *Curr. Biol.*, vol. 22, no. 17, pp. R753–R761, Sep. 2012.

[12] Biomarkers Definitions Working Group., “Biomarkers and surrogate endpoints: Preferred definitions and conceptual framework,” *Clin. Pharmacol. Ther.*, vol. 69, no. 3, pp. 89–95, Mar. 2001.

[13] J. Nyhlén, R. Constantinescu, and H. Zetterberg, “Problems associated with fluid biomarkers for Parkinson’s disease,” *Biomark. Med.*, vol. 4, no. 5, pp. 671–681, Oct. 2010.

[14] M. M. Mielke and W. Maetzler, “A ‘bird’s eye’ view on the current status and potential benefits of blood biomarkers for Parkinson’s disease,” *Biomark. Med.*, vol. 8, no. 2, pp. 225–227, Feb. 2014.

[15] S. Sharma *et al.*, “Biomarkers in Parkinson’s disease (recent update),” *Neurochem. Int.*, vol. 63, no. 3, pp. 201–229, Sep. 2013.

[16] Ali, “Biosensors: Their Fundamentals, Designs, Types and Most Recent Impactful Applications: A Review,” *J Biosens Bioelectron*, vol. 8, no. 8, 2017.

[17] M. Nič, J. Jirát, B. Košata, A. Jenkins, and A. McNaught, Eds., *IUPAC Compendium of Chemical Terminology*. Research Triagle Park, NC: IUPAC, 2009.

[18] V. Perumal and U. Hashim, “Advances in biosensors: Principle, architecture and applications,” *J. Appl. Biomed.*, vol. 12, no. 1, pp. 1–15, Jan. 2014.

[19] G. K. Knopf and A. S. Bassi, *Smart biosensor technology*. CRC Press/Taylor & Francis, 2007.

[20] D. R. The Â Venot *et al.*, “Electrochemical biosensors: Recommended definitions and classification (Technical Report),” *Pure Appl. Chem*, vol. 71, no. 12, pp. 2333–2348, 1999.

[21] R. Monošík, M. Streďanský, and E. Šturdík, “Biosensors - classification, characterization and new trends,” *Acta Chim. Slovaca*, vol. 5, no. 1, Jan. 2012.

[22] N. Bhalla, P. Jolly, N. Formisano, and P. Estrela, “Introduction to biosensors,” *Essays Biochem.*, vol. 60, pp. 1–8, 2016.

[23] J. Lin and H. Ju, “Electrochemical and chemiluminescent immunosensors for tumor markers,” *Biosens. Bioelectron.*, vol. 20, no. 8, pp. 1461–1470, Feb. 2005.

[24] T. R. J. Holford, F. Davis, and S. P. J. Higson, “Recent trends in antibody based sensors,” *Biosens. Bioelectron.*, vol. 34, no. 1, pp. 12–24, Apr. 2012.

[25] K. R. Rogers, “Principles of affinity-based biosensors,” vol. 14, no. 2. pp. 109–129, 2000.

[26] S. Guo and S. Dong, “Biomolecule-nanoparticle hybrids for electrochemical biosensors,” *TrAC Trends Anal. Chem.*, vol. 28, no. 1, pp. 96–109, Jan. 2009.

[27] M. Pan, Y. Gu, Y. Yun, M. Li, X. Jin, and S. Wang, “Nanomaterials for electrochemical immunosensing,” *Sensors (Switzerland)*, vol. 17, no. 5, 2017.

[28] K. L. Adams, M. Puchades, and A. G. Ewing, “In Vitro Electrochemistry of Biological Systems.,” *Annu. Rev. Anal. Chem. (Palo Alto. Calif).*, vol. 1, p. 329, Jul. 2008.

[29] Yanhui Zhang, and Bo Zhang, and H. S. White*, “Electrochemistry of Nanopore Electrodes in Low Ionic Strength Solutions,” 2006.

[30] F. Wang and S. Hu, “Electrochemical sensors based on metal and semiconductor nanoparticles,” *Microchim. Acta*, vol. 165, no. 1–2, pp. 1–22, Apr. 2009.

[31] J. M. Pingarrón, P. Yáñez-Sedeño, and A. González-Cortés, “Gold nanoparticle-based electrochemical biosensors,” *Electrochim. Acta*, vol. 53, no. 19, pp. 5848–5866, 2008.

[32] P. Yáñez-Sedeño and J. M. Pingarrón, “Gold nanoparticle-based electrochemical biosensors,” *Anal. Bioanal. Chem.*, vol. 382, no. 4, pp. 884–886, Jun. 2005.

[33] S. Liu, N. Leech, H. Ju, and P. Huangxian Ju, “Application of Colloidal Gold in Protein Immobilization, Electron Transfer, and Biosensing,” *NY 10016 Anal. Lett.*, vol. 36, no. 1, pp. 1–19, 2003.

[34] M. H. Rashid, R. R. Bhattacharjee, A. Kotal, and T. K. Mandal, “Synthesis of Spongy Gold Nanocrystals with Pronounced Catalytic Activities,” *Langmuir*, vol. 22, no. 17, pp. 7141–7143, Aug. 2006.

[35] J. Turkevich, P. C. Stevenson, and J. Hillier, “A study of the nucleation and growth processes in the synthesis of colloidal gold,” *Discuss. Faraday Soc.*, vol. 11, no. 0, pp. 55–75, 1951.

[36] M. Sireesha, V. Jagadeesh Babu, A. S. Kranthi Kiran, and S. Ramakrishna, “A review on carbon nanotubes in biosensor devices and their applications in medicine,” *Nanocomposites*, vol. 4, no. 2, pp. 36–57, 2018.

[37] G. Herlem, F. Picaud, C. Girardet, and O. Micheau, “Carbon Nanotubes: Synthesis,

Characterization, and Applications in Drug-Delivery Systems," *Nanocarriers Drug Deliv.*, pp. 469–529, Jan. 2019.

[38] A. M. Holban and E. Andronescu, "Inorganic nanoarchitectonics designed for drug delivery and anti-infective surfaces," *Surf. Chem. Nanobiomaterials*, pp. 301–327, Jan. 2016.

[39] B. Peng *et al.*, "Measurements of near-ultimate strength for multiwalled carbon nanotubes and irradiation-induced crosslinking improvements," *Nat. Nanotechnol.*, vol. 3, no. 10, pp. 626–631, Oct. 2008.

[40] B. Q. Wei, R. Vajtai, and P. M. Ajayan, "Reliability and current carrying capacity of carbon nanotubes," *Appl. Phys. Lett.*, vol. 79, no. 8, pp. 1172–1174, Aug. 2001.

[41] †,‡ Eric Pop, † David Mann, † Qian Wang, ‡ and Kenneth Goodson, and † Hongjie Dai*, "Thermal Conductance of an Individual Single-Wall Carbon Nanotube above Room Temperature," 2005.

[42] I. H. Cho *et al.*, "Current technologies of electrochemical immunosensors: Perspective on signal amplification," *Sensors (Switzerland)*, vol. 18, no. 1. 2018.

[43] D. Hutanu, M. D Frishberg, L. Guo, and and C. C. Darie, "Recent Applications of Polyethylene Glycols (PEGs) and PEG Derivatives," *Mod. Chem. Appl.*, vol. 02, no. 02, pp. 2–7, 2014.

[44] M. Rizwan, M. Hazmi, S. A. Lim, and M. U. Ahmed, "A highly sensitive electrochemical detection of human chorionic gonadotropin on a carbon nano-onions/gold nanoparticles/polyethylene glycol nanocomposite modified glassy carbon electrode," *J. Electroanal. Chem.*, vol. 833, pp. 462–470, Jan. 2019.

[45] F. M. Veronese and G. Pasut, "PEGylation, successful approach to drug delivery," *Drug Discov. Today*, vol. 10, no. 21, pp. 1451–1458, Nov. 2005.

[46] L. Tian *et al.*, "Bioplasmonic calligraphy for multiplexed label-free biodetection," *Biosens. Bioelectron.*, vol. 59, pp. 208–215, Sep. 2014.

[47] D. W. Baker *et al.*, "Development of optical probes for in vivo imaging of polarized macrophages during foreign body reactions," *Acta Biomater.*, vol. 10, no. 7, pp. 2945–2955, Jul. 2014.

[48] H.-B. Pang *et al.*, "A free cysteine prolongs the half-life of a homing peptide and improves its tumor-penetrating activity," *J. Control. Release*, vol. 175, pp. 48–53, Feb. 2014.

[49] M. Moreno, E. Zurita, and E. Giralt, "Delivering wasp venom for cancer therapy," *J. Control. Release*, vol. 182, pp. 13–21, May 2014.

[50] E. H. Nguyen, M. R. Zanotelli, M. P. Schwartz, and W. L. Murphy, "Differential effects of cell adhesion, modulus and VEGFR-2 inhibition on capillary network formation in synthetic hydrogel arrays," *Biomaterials*, vol. 35, no. 7, pp. 2149–2161, Feb. 2014.

[51] F. Peng *et al.*, "PEGylation of G-CSF in organic solvent markedly increase the efficacy and reactivity through protein unfolding, hydrolysis inhibition and solvent effect.," *J. Biotechnol.*, vol. 170, pp. 42–9, Jan. 2014.

[52] "PEGylation Technology - Creative PEGWorks." [Online]. Available: https://www.creativepegworks.com/technology.html. [Accessed: 28-May-2019].

[53] J. A. Ho *et al.*, "Diagnostic Detection of Human Lung Cancer-Associated Antigen Using a Gold Nanoparticle-Based Electrochemical Immunosensor," *Anal. Chem.*, vol. 82, no. 14, pp. 5944–5950, Jul. 2010.

[54] D. K. Male, *Immunology*. Elsevier/Saunders, 2013.

[55] J. M. Fowler, D. K. Y. Wong, H. B. Halsall, and W. R. Heineman, "CHAPTER 5 - Recent developments in electrochemical immunoassays and immunosensors," in

Electrochemical Sensors, Biosensors and their Biomedical Applications, X. Zhang, H. Ju, and J. Wang, Eds. San Diego: Academic Press, 2008, pp. 115–143.

[56] george L. Kumar *et al.*, "Immunohistochemical (IHC) Staining Methods," 2009.

[57] B. Byrne, E. Stack, N. Gilmartin, and R. O'Kennedy, "Antibody-based sensors: Principles, problems and potential for detection of pathogens and associated toxins," *Sensors (Switzerland)*, vol. 9, no. 6, pp. 4407–4445, 2009.

[58] E. K. Wujcik *et al.*, "Antibody nanosensors: a detailed review," *RSC Adv.*, vol. 4, no. 82, pp. 43725–43745, Sep. 2014.

[59] T. K. CHRISTOPOULOS and E. P. DIAMANDIS, "10 - Immunoassay Configurations," in *Immunoassay*, E. P. Diamandis and T. K. Christopoulos, Eds. San Diego: Academic Press, 1996, pp. 227–236.

[60] D. Tang, R. Yuan, and Y. Chai, "Ultrasensitive Electrochemical Immunosensor for Clinical Immunoassay Using Thionine-Doped Magnetic Gold Nanospheres as Labels and Horseradish Peroxidase as Enhancer," *Anal. Chem.*, vol. 80, no. 5, pp. 1582–1588, 2008.

[61] X. Pei, B. Zhang, J. Tang, B. Liu, W. Lai, and D. Tang, "Sandwich-type immunosensors and immunoassays exploiting nanostructure labels: A review," *Anal. Chim. Acta*, vol. 758, pp. 1–18, 2013.

[62] S. K. Vashist and J. H. T. Luong, *Antibody Immobilization and Surface Functionalization Chemistries for Immunodiagnostics*. Elsevier Inc., 2018.

[63] N. G. Welch, J. A. Scoble, B. W. Muir, and P. J. Pigram, "Orientation and characterization of immobilized antibodies for improved immunoassays (Review)," *Biointerphases*, vol. 12, no. 2, p. 02D301, 2017.

[64] J. E. Butler *et al.*, "The immunochemistry of sandwich elisas—VI. Greater than 90% of monoclonal and 75% of polyclonal anti-fluorescyl capture antibodies (CAbs) are denatured by passive adsorption," *Mol. Immunol.*, vol. 30, no. 13, pp. 1165–1175, Sep. 1993.

[65] Y. Liu and J. Yu, "Oriented immobilization of proteins on solid supports for use in biosensors and biochips: a review," *Microchim. Acta*, vol. 183, no. 1, pp. 1–19, Jan. 2016.

[66] X. Zhang, H. Ju, and J. Wang, *Electrochemical sensors, biosensors and their biomedical applications*. Academic Press, 2007.

[67] J. L. Acero Sánchez, A. Fragoso, H. Joda, G. Suárez, C. J. McNeil, and C. K. O'Sullivan, "Site-directed introduction of disulfide groups on antibodies for highly sensitive immunosensors," *Anal. Bioanal. Chem.*, vol. 408, no. 19, pp. 5337–5346, Jul. 2016.

[68] A. Hasan and L. M. Pandey, "Review: Polymers, Surface-Modified Polymers, and Self Assembled Monolayers as Surface-Modifying Agents for Biomaterials," *Polym. Plast. Technol. Eng.*, vol. 54, no. 13, pp. 1358–1378, Sep. 2015.

[69] † Shengfu Chen, ‡ Lingyun Liu, † and Jian Zhou, and † Shaoyi Jiang*, "Controlling Antibody Orientation on Charged Self-Assembled Monolayers," 2003.

[70] J. C. Love, L. A. Estroff, J. K. Kriebel, R. G. Nuzzo, and G. M. Whitesides, "Self-Assembled Monolayers of Thiolates on Metals as a Form of Nanotechnology," *Chem. Rev.*, vol. 105, no. 4, pp. 1103–1170, Apr. 2005.

[71] S. C. B. Gopinath, T. Tang, M. Citartan, and Y. Chen, "Biosensors and Bioelectronics Current aspects in immunosensors," *Biosens. Bioelectron.*, vol. 57, pp. 292–302, 2014.

[72] R. Danczyk, B. Krieder, A. North, T. Webster, H. HogenEsch, and A. Rundell, "Comparison of antibody functionality using different immobilization methods," *Biotechnol. Bioeng.*, vol. 84, no. 2, pp. 215–223, Oct. 2003.

[73] E. J. Franco, H. Hofstetter, and O. Hofstetter, "A comparative evaluation of random and site-specific immobilization techniques for the preparation of antibody-based chiral

stationary phases.," *J. Sep. Sci.*, vol. 29, no. 10, pp. 1458–69, Jul. 2006.

[74] M. Masařík *et al.*, "Sensitive Electrochemical Detection of Native and Aggregated α-Synuclein Protein Involved in Parkinson's Disease," *Electroanalysis*, vol. 16, no. 13-14, pp. 1172–1181, Jul. 2004.

[75] D. A. Yushchenko, J. A. Fauerbach, S. Thirunavukkuarasu, E. A. Jares-Erijman, and T. M. Jovin, "Fluorescent Ratiometric MFC Probe Sensitive to Early Stages of α-Synuclein Aggregation," *J. Am. Chem. Soc.*, vol. 132, no. 23, pp. 7860–7861, Jun. 2010.

[76] M. Dragusanu, B.-A. Petre, S. Slamnoiu, C. Vlad, T. Tu, and M. Przybylski, "On-Line Bioaffinity-Electrospray Mass Spectrometry for Simultaneous Detection, Identification, and Quantification of Protein–Ligand Interactions," *J. Am. Soc. Mass Spectrom.*, vol. 21, no. 10, pp. 1643–1648, 2010.

[77] D. Lee, Y.-J. Choe, M. Lee, D. H. Jeong, and S. R. Paik, "Protein-Based SERS Technology Monitoring the Chemical Reactivity on an α-Synuclein-Mediated Two-Dimensional Array of Gold Nanoparticles," *Langmuir*, vol. 27, no. 21, pp. 12782–12787, Nov. 2011.

[78] K. Sun, N. Xia, L. Zhao, K. Liu, W. Hou, and L. Liu, "Aptasensors for the selective detection of alpha-synuclein oligomer by colorimetry, surface plasmon resonance and electrochemical impedance spectroscopy," *Sensors Actuators, B Chem.*, vol. 245, pp. 87–94, 2017.

[79] S. M. Taghdisi *et al.*, "A novel electrochemical aptasensor based on nontarget-induced high accumulation of methylene blue on the surface of electrode for sensing of α-synuclein oligomer," *Biosens. Bioelectron.*, vol. 123, no. July 2018, pp. 14–18, 2019.

[80] M. N. S. Karaboğa and M. K. Sezgintürk, "Cerebrospinal fluid levels of alpha-synuclein measured using a poly-glutamic acid-modified gold nanoparticle-doped disposable neuro-biosensor system," *Analyst*, 2018.

[81] Y. An *et al.*, "Sensitive electrochemical immunosensor for α-synuclein based on dual signal amplification using PAMAM dendrimer-encapsulated Au and enhanced gold nanoparticle labels," *Biosens. Bioelectron.*, vol. 32, no. 1, pp. 224–230, 2011.

[82] Y. An *et al.*, "A photoelectrochemical immunosensor based on au-doped TiO2nanotube arrays for the detection of α-synuclein," *Chem. - A Eur. J.*, vol. 16, no. 48, pp. 14439–14446, 2010.

[83] N. Elgrishi, K. J. Rountree, B. D. McCarthy, E. S. Rountree, T. T. Eisenhart, and J. L. Dempsey, "A Practical Beginner's Guide to Cyclic Voltammetry," *J. Chem. Educ.*, vol. 95, no. 2, pp. 197–206, 2018.

[84] A. B. Bocarsly, "Electrochemical Techniques, Introduction," in *Characterization of Materials*, Hoboken, NJ, USA: John Wiley & Sons, Inc., 2012, pp. 1–3.

[85] B. Uslu and S. A. Ozkan, "Electroanalytical Methods for the Determination of Pharmaceuticals: A Review of Recent Trends and Developments," *Anal. Lett.*, vol. 44, no. 16, pp. 2644–2702, Nov. 2011.

[86] C. G. Zoski, *Handbook of electrochemistry*. Elsevier, 2007.

[87] G. Mehmet, "The Role of and the Place of Method Validation in Drug Analysis Using Electroanalytical Techniques," *Open Anal. Chem. J.*, vol. 5, no. 1, pp. 1–21, Jan. 2011.

[88] A. J. Bard and L. R. Faulkner, *Electrochemical methods : fundamentals and applications*. Wiley, 2001.

[89] K. Izutsu, *Electrochemistry in Nonaqueous Solutions*. Weinheim, Germany: Wiley-VCH Verlag GmbH & Co. KGaA, 2009.

[90] M. Lovrić, "Square-Wave Voltammetry," in *Electroanalytical Methods*, Berlin, Heidelberg: Springer Berlin Heidelberg, 2005, pp. 111–136.

[91] V. Mirceski, R. Gulaboski, M. Lovric, I. Bogeski, R. Kappl, and M. Hoth, "Square-Wave

Voltammetry: A Review on the Recent Progress," 2013.

[92] F. Lisdat and D. Schäfer, "The use of electrochemical impedance spectroscopy for biosensing."

[93] T. Ikeda and K. Kano, "An electrochemical approach to the studies of biological redox reactions and their applications to biosensors, bioreactors, and biofuel cells," *J. Biosci. Bioeng.*, vol. 92, no. 1, pp. 9–18, Jan. 2001.

[94] U. Retter and H. Lohse, "Electrochemical Impedance Spectroscopy," in *Electroanalytical Methods*, Berlin, Heidelberg: Springer Berlin Heidelberg, 2010, pp. 159–177.

[95] N. Nhs, "Description : Handling and Use : Storage Conditions : Product Structure : Related Products : Product Specifications : To Order :," vol. 1, no. 800. p. 4221, 2000.

[96] J. Kimling, M. Maier, B. Okenve, V. Kotaidis, H. Ballot, and A. Plech, "Turkevich Method for Gold Nanoparticle Synthesis Revisited," *J. Phys. Chem. B*, vol. 110, no. 32, pp. 15700–15707, Aug. 2006.

[97] D. A. Armbruster and T. Pry, "Limit of blank, limit of detection and limit of quantitation.," *Clin. Biochem. Rev.*, vol. 29 Suppl 1, no. Suppl 1, pp. S49–52, Aug. 2008.

[98] H. A. O. Hill, C. B. Moore, and D. M. A. NabiRahni, "Electrochemistry of redox proteins," in *Bioelectrochemistry of Biomacromolecules*, Basel: Birkhäuser Basel, 1997, pp. 183–204.

[99] F. O. Gomes *et al.*, "Biosensor for direct bioelectrocatalysis detection of nitric oxide using nitric oxide reductase incorporated in carboxylated single-walled carbon nanotubes / lipidic 3 bilayer nanocomposite," *Bioelectrochemistry*, vol. 127, pp. 76–86, 2019.

[100] G. T. Hermanson, "Chapter 11 - Biotinylation Reagents," in *Elsevier Science*, G. T. B. T.-B. T. (Second E. Hermanson, Ed. New York: Academic Press, 2008, pp. 506–545.